

AEP REACTOR CORE THERMAL-HYDRAULIC ANALYSIS  
USING THE  
COBRA IIIC/MIT-2 COMPUTER CODE

BY  
R. S. SHARMA

NUCLEAR FUEL AND ANALYSIS SECTION

AMERICAN ELECTRIC POWER SERVICE CORPORATION  
COLUMBUS, OHIO

NOVEMBER 1988

APPROVED BY

*D. H. Malin* 11/10/88

D. H. MALIN  
MANAGER  
NUCLEAR FUEL AND  
ANALYSIS SECTION

8902080038 890208  
PDR ADOCK 05000315  
P PDC

## ABSTRACT

The American Electric Power (AEP) Service Corporation has developed the thermal-hydraulic analysis capabilities using COBRA IIIC/MIT-2 computer code to analyze the core conditions of the Donald C. Cook Nuclear Plant. This methodology is based on the single stage method in which an array of subchannel representing the hot assembly is combined with an array of lumped channels representing the remaining assemblies of the core segment. The thermal and hydraulic models have been developed. Engineering uncertainties are applied to the hot channel and the hot fuel rod.

The thermal-hydraulic model has been used to determine the hot channel fluid conditions and the resulting minimum departure from nucleate boiling ratio (MDNBR). The accuracy of the model has been verified through comparisons with steady state and transient analyses used in the design and licensing documents. These comparisons show that the results obtained using AEP methods are in excellent agreement with those presented in the licensing documents.

#### ACKNOWLEDGEMENTS

I am thankful to Mr. J.M. Cleveland for his encouragement given to me during the development of this work. Thanks to Professor N. E. Todreas of the Massachusetts Institute of Technology for kindly providing to us the COBRA IIIC/MIT-2 Computer program. Assistance of Mr. D. A. Kester in performing the methodology verification is thankfully acknowledged. Thanks to Ms. Sheri Ellis for typing this report.

## TABLE OF CONTENTS

	<u>Page</u>
ABSTRACT .....	(i)
ACKNOWLEDGEMENTS .....	(ii)
TABLE OF CONTENTS .....	(iii)
LIST OF FIGURES .....	(v)
LIST OF TABLES .....	(vi)
SECTION 1-INTRODUCTION .....	1-1
SECTION 2-COBRA IIIC/MIT-2 COMPUTER CODE DESCRIPTION .....	2-1
2.1 Introduction .....	2-1
2.2 Description of COBRA IIIC/MIT-2 Computer Code .....	2-1
2.3 Correlations and Models Used .....	2-3
2.3.1 Friction Factor .....	2-3
2.3.2 Void Fraction .....	2-4
2.3.3 Single and Two-phase Turbulent Mixing .....	2-4
2.3.4 Critical Heat Flux Correlation .....	2-4
2.4 Input Parameters .....	2-5
SECTION 3-HYDRAULIC MODEL DESCRIPTION .....	3-1
3.1 Introduction .....	3-1
3.2 General Description of the Cook, Unit 1 Core .....	3-1
3.3 One-Eighth Core Representation .....	3-2
SECTION 4-THERMAL MODEL DESCRIPTION .....	4-1
4.1 Introduction .....	4-1
4.2 General Description of the Thermal Design of Cook, Unit 1 Core .....	4-3
4.3 Inlet Flow Distribution .....	4-3

	<u>Page</u>
4.4 Radial Power Distribution .....	4-4
4.5 Axial Power Distribution .....	4-5
4.6 Reactor Operating Conditions .....	4-6
4.7 Forcing Functions for Transient Analysis .....	4-7
SECTION 5-ENGINEERING UNCERTAINTIES .....	5-1
5.1 Introduction .....	5-1
5.2 Heat Flux Engineering Subfactor, $F_q^E$ .....	5-1
5.3 Enthalpy Rise Engineering Subfactor, $F_{\Delta H}^E$ .....	5-2
SECTION 6-THERMAL-HYDRAULIC MODEL VERIFICATION .....	6-1
6.1 Introduction .....	6-1
6.2 Steady State Analysis .....	6-1
6.2.1 Surry core Analysis at 100% Power Performed by VEPCO .....	6-1
6.2.2 Three-Loop Westinghouse PWR Analysis at 118% Power Performed by ANF .....	6-2
6.2.3 Cook, Unit 1 FSAR Analysis at 100% Power .....	6-2
6.3 Transient Analysis .....	6-3
6.3.1 Excessive Load Increase Transient .....	6-3
6.3.2 Uncontrolled Control Rod Assembly Withdrawal at Power Transient .....	6-4
6.3.3 Complete Loss of Reactor Coolant Flow Transient .....	6-4
SECTION 7-SUMMARY AND CONCLUSIONS .....	7-1
SECTION 8-REFERENCES .....	8-1

## LIST OF FIGURES

Figure	Title	Page
3-1	Fuel Assembly Arrangement of Unit 1 of Donald C. Cook Plant .....	3-9
3-2	Cross-sectional View of Cook, Unit 1 Fuel Assembly .....	3-10
3-3	Side View of Cook, Unit 1 Fuel Assembly .....	3-11
3-4	One-eight Assembly Geometry of 58 Ch. Model .	3-12
3-5	Subchannel Geometry of 58 Channel Model .....	3-13
4-1	Inlet Flow Distribution of 58 Channel Model..	4-8
4-2	Assembly Power Distribution of 58 Channel Model.....	4-9
4-3	Subchannel Power Distribution of 58 Channel Model .....	4-10
6-1	Assembly Power Distribution for 53 Channel Model for Surry Core .....	6-12
6-2	Subchannel Power Distribution .....	6-13
6-3	Assembly Power Distribution for 58 Channel Model for Cook, Unit 1 Core .....	6-14
6-4	DNBR versus Time for Excessive Load Increase Transient .....	6-15
6-5	DNBR versus Time for Uncontrolled Control Rod Assembly Withdrawal at Power Transient ..	6-16
6-6	DNBR versus Time for Complete Loss of Reactor coolant Flow Transient .....	6-17

## LIST OF TABLES

Table	Title	Page
2-1	Input Parameters .....	2-6
3-1	Assembly Hydraulic Parameter .....	3-4
3-2	Axial Positions of Assembly Components .....	3-5
3-3	Assembly Hydraulic Data .....	3-6
3-4	Perimeter cell Hydraulic Data .....	3-6
3-5	Corner Cell Hydraulic Data .....	3-7
3-6	Thimble Cell Hydraulic Data .....	3-7
3-7	Unit Cell Hydraulic Data .....	3-8
6-1	Listing of AEP Verification Analyses .....	6-6
6-2	Reactor Conditions for Surry Core Analysis .	6-7
6-3	Axial Power Distribution for Surry Core Analysis .....	6-8
6-4	Reactor Conditions for 3-Loop Westinghouse PWR Analysis .....	6-9
6-5	Reactor Conditions for Cook, Unit 1 FSAR Steady State Analysis .....	6-10
6-6	Axial Power Distribution for Cook, Unit 1 Core Analysis .....	6-11
7-1	Summary of Comparisons .....	7-1

## SECTION 1

### INTRODUCTION

The core thermal-hydraulic analysis is performed to calculate the coolant conditions in order to verify that the fuel assemblies of the core can safely meet the limitations imposed by departure from nucleate boiling (DNB). DNB, which could occur on the fuel heating surface, is characterized by a sudden decrease in heat transfer coefficient with a corresponding increase in the surface temperature. DNB is one of the fuel design criterion because of the possibility of fuel rod failure resulting from the increased temperature.

In order to avoid the potential DNB related fuel damage, a design basis is established in terms of minimum departure from nucleate boiling ratio (MDNBR). DNBR is defined as a ratio of the critical heat flux to the local heat flux. A design DNBR limit is imposed on fuel in order to ensure that adequate heat transfer between fuel cladding and reactor coolant takes place. A value of DNBR greater than the design limit indicates that a safety margin to the thermal limits within the core exists. The core thermal-hydraulic analysis performs the accurate calculations of DNBRs to quantify the core thermal margin.

In performing the thermal-hydraulic analysis, a subchannel approach is used in which a section of the core is modeled as an array of adjoining subchannels. These subchannels may be formed either by four neighboring rods in a square fuel rod lattice or three neighboring rods in a triangular lattice. One of the channels is given the highest integrated power by assigning the design radial and axial power distributions to all the four fuel rods forming that channel. This channel is called the hot channel. Engineering uncertainties are applied to the hot channel and the hot fuel rods in order to account for the effects of flow conditions and manufacturing tolerances used in fuel fabrication. A detailed thermal analysis of the core is then performed to determine the flows and enthalpies at each axial position within the hot channel.

The American Electric Power (AEP) Service Corporation has used the single stage method<sup>(1)</sup> to perform the thermal-hydraulic analysis of Unit 1, Cycle 1 of the Donald C. Cook Nuclear Plant. This method has been used previously<sup>(2)</sup> for DNB analysis. In this method an array of subchannel representing the hot assembly is combined with an array of lumped channels representing the remaining assemblies of the core segment. The accuracy of this approach has been verified through comparisons with analyses performed by others<sup>(2,3)</sup>, and those used in the designing and licensing of Unit 1 of Cook Plant.<sup>(4)</sup> The steady state and transient results using AEP methodology are in excellent agreement with those presented in Unit 1 Final Safety Analysis Report.<sup>(4)</sup>

This report describes the AEP thermal-hydraulic model and presents the results and comparisons which demonstrate the accuracy of the model. Section 2 describes the COBRA IIIC/MIT-2 computer code and various correlations/options used in the analysis. The hydraulic and thermal models are described in Sections 3 and 4, respectively. The engineering uncertainties applied to the thermal-hydraulic model are briefly described in Section 5. Section 6 describes the specific analyses performed and comparisons of AEP results made with licensing documents. Conclusions are provided in Section 7.

## SECTION 2

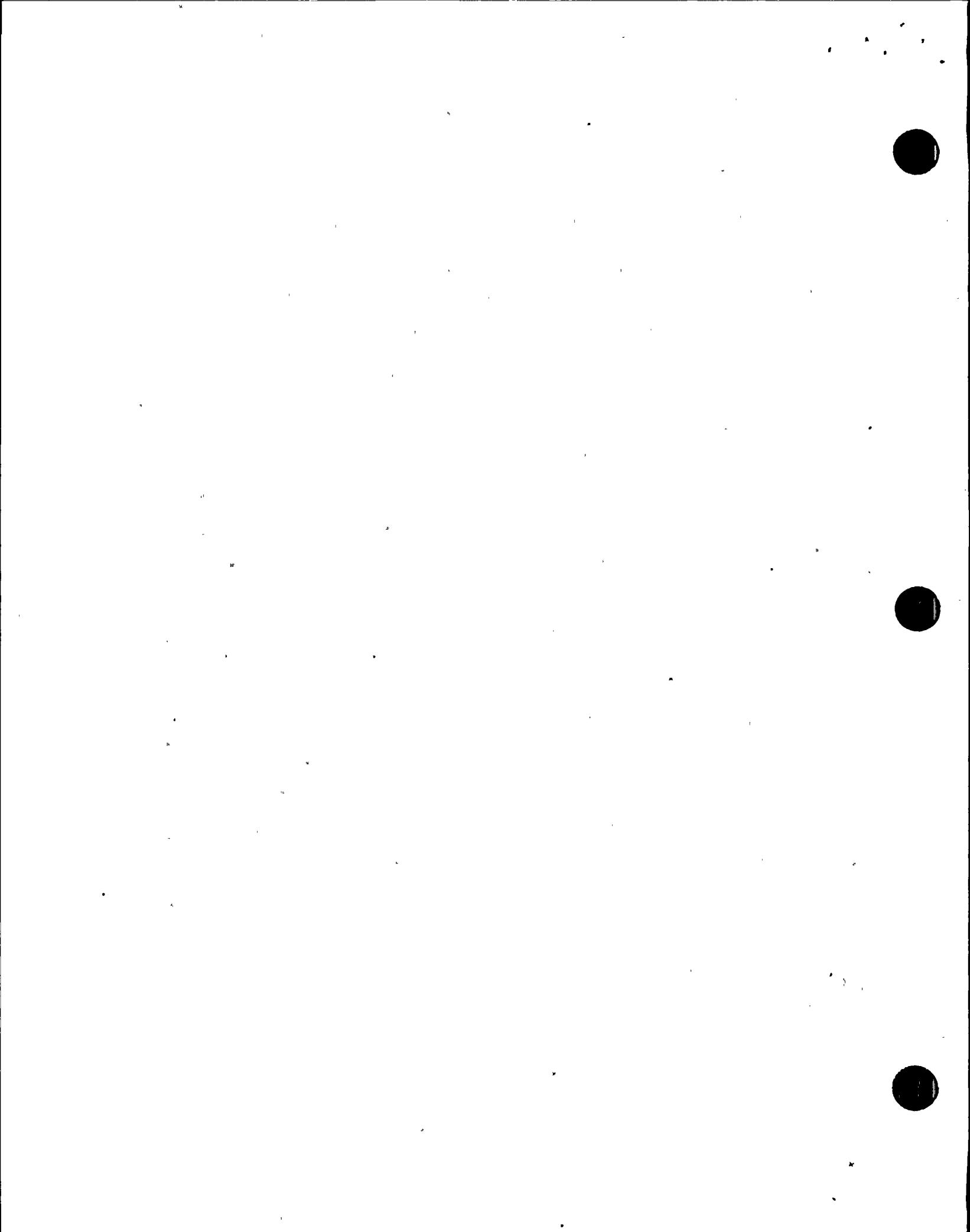
### COBRA IIIC/MIT-2 COMPUTER CODE DESCRIPTION

#### 2.1 Introduction

The COBRA IIIC/MIT-2 computer code <sup>(5)</sup> has been developed by the Massachusetts Institute of Technology. The structure of this code is based on COBRA IIIC computer code. <sup>(6)</sup> However, COBRA IIIC/MIT-2 computer code runs faster and has the capabilities to handle larger core geometries. In addition, the code includes the effects of crossflow mixing. Because of these features, the COBRA IIIC/MIT-2 code has been used in the development of AEP Thermal-Hydraulic Methodology. A brief description of the code and various models used are given in the following sections:

#### 2.2 Description of COBRA IIIC/MIT-2 Computer Code

The COBRA IIIC/MIT-2 computer code computes the flow and enthalpy within interconnected flow channels using finite difference equations. The mathematical model considers both turbulent and diversion crossflow mixing between subchannels.- Each subchannel is assumed to contain one-dimensional, two-phase, separated slip flow. The two-phase flow structure is assumed to be fine enough to define the void fraction as a function of enthalpy, flow-rate, heat flux, pressure, position and time. The two-phase flow correlations are assumed to apply to transients. Sonic velocity propagation effects were neglected.



The constitutive equations are solved as a boundary-value problem by using the semi-explicit finite difference technique. The boundary conditions used are inlet enthalpy, inlet flow, inlet crossflow, and exit pressure. Initial conditions used in the solution are established from initial steady-state calculations. When performing a computation, the code iterates over the length of the core until convergence of the flow solution is obtained.

The same mathematical model is used for both steady state and transient computation. Steady state calculations are performed first to obtain the initial conditions for the transient calculations. For steady state calculations, a large value for  $\Delta t$  is set, since the constitutive equations are stable for large time step. An iteration is performed until convergence of the flow solution is obtained. Convergence is achieved when the change in any subchannel flow is less than a user specified fraction of the flow from the previous iteration.

The above procedure is used for transient calculations but for a user selected time step  $\Delta t$ . Boundary conditions and other forcing functions are set to their desired values at the new time. The calculations are performed along the channel length until the convergence on the crossflow is achieved. The converged solution is used as the initial conditions for the next time step. The procedure continues for all time steps.

The set of continuity, momentum, and energy equations form the basic structure of the mathematical model, however, the final solution still depends on the use of empirical correlations. The



correlations which have been selected for use in AEP thermal-hydraulic model are described in the following section.

### 2.3 Correlations and Models Used

#### 2.3.1 Friction Factor

The single and two-phase pressure drops are calculated by using the isothermal friction factor correlation given by the following equation. (5)

$$f_{iso} = a (Re)^b + c$$

Where Re is the Reynolds number. The values used in the model are  $a = 0.2$ ,  $b = -0.2$  and  $c = 0$ . It was assumed that all the subchannels have same roughness and pitch-to-diameter ratio, and hence the same friction factor.

The friction factor can be corrected for wall viscosity by using the correlation (7)

$$\frac{f}{f_{iso}} = 1 + \frac{P_h}{P_w} \left[ \left( \frac{\mu_{wall}}{\mu_{bulk}} \right)^{0.6} - 1 \right]$$

where  $P_h$  is heated perimeter,  $P_w$  is wetted perimeter,  $\mu_{bulk}$  is the viscosity evaluated at the bulk fluid temperature  $T_{bulk}$ ,  $\mu_{wall}$  is the viscosity at wall temperature which is calculated from

$$T_{wall} = T_{bulk} + (q''/h)$$

where  $q''$  is the surface heat flux. The heat transfer coefficient,  $h$  is calculated from the Dittus-Boelter correlation (8) at bulk fluid properties. No wall viscosity correction was used in our model.

In two-phase flow region, the homogeneous model was used,  
i.e.,

$$\phi = 1.0 \quad x < 0$$

$$\phi = \rho_f / \rho \quad x > 0$$

where  $\phi$  is two-phase friction multiplier,  $x$  is quality,  $\rho_f$  is liquid density, and  $\rho$  is two-phase density calculated by

$$\rho = \rho_g \alpha + \rho_f (1 - \alpha)$$

where  $\rho_g$  is saturated vapor density and  $\alpha$  is void fraction.

### 2.3.2 Void Fraction

The void fraction of the flow was calculated using Levy's subcooled void fraction model.<sup>(9)</sup> Levy's model calculates the true quality in terms of the equilibrium quality and the quality at which bubble departure starts. The void fraction is calculated by using the homogeneous model<sup>(9)</sup> with slip ratio set equal to 1.0.

### 2.3.3 Single and Two-Phase Turbulent Mixing

The single and two-phase turbulent crossflow between adjacent channels is calculated using<sup>(6)</sup>

$$W'_k = \beta s_k G$$

where  $W'_k$  is the turbulent crossflow rate between adjacent channel per axial length,  $\beta$  is the mixing coefficient,  $s_k$  is the common gap and  $G$  is the average mass velocity of the adjacent channel. As a simple case  $\beta$  was set equal to 0.02.

### 2.3.4 Critical Heat Flux Correlation

In order to verify the methodology, the W-3 correlation in conjunction with F-factor correction is used for calculating the non-uniform heat flux. The grid and unheated wall correction factors are applied to predict the critical heat flux. Other critical heat flux correlations are available and may be used for a particular application with appropriate justification.

#### 2.4 Input Parameters

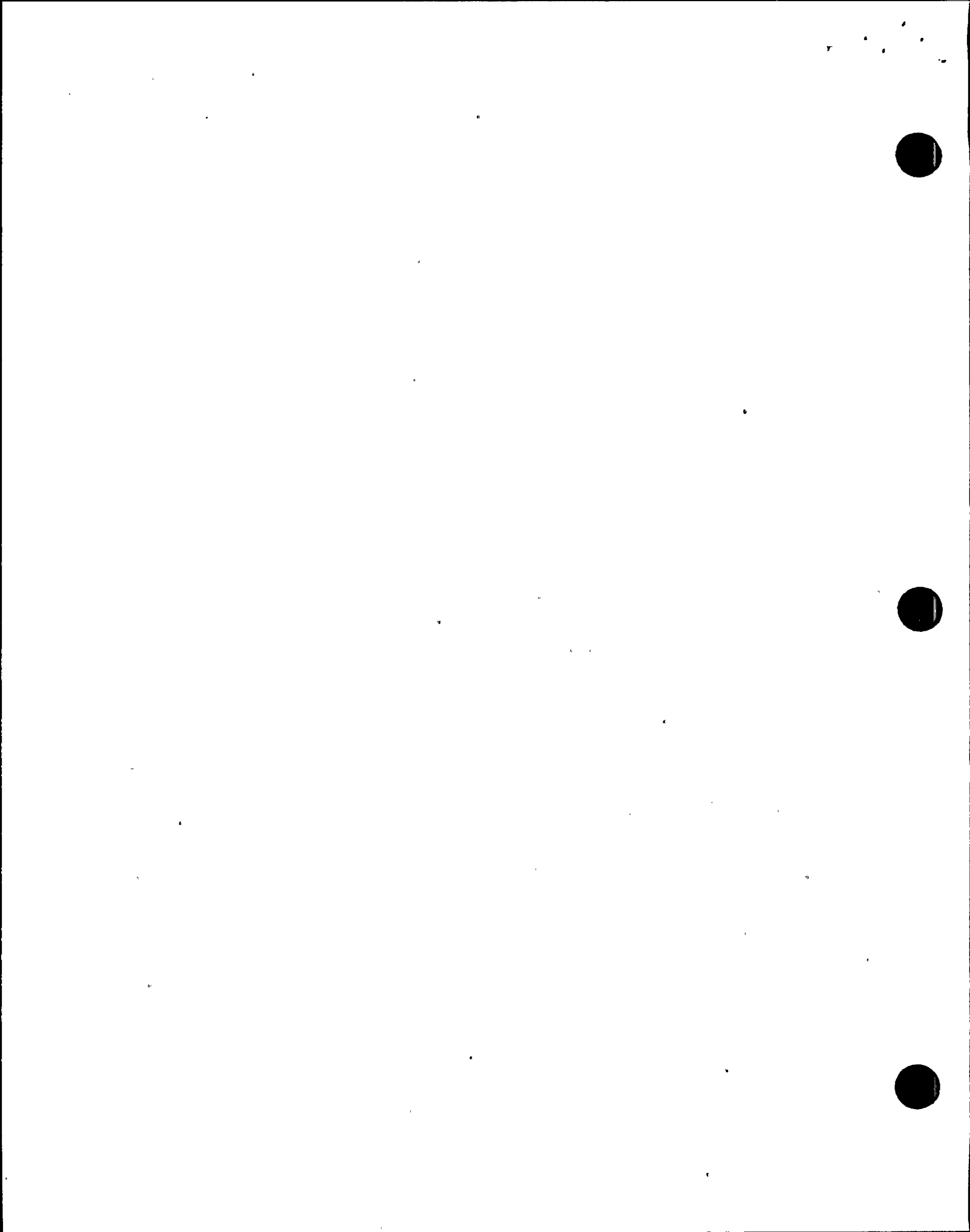
The input parameters used in the D.C. Cook, Unit 1 analysis are listed in Table 2-1. The number of axial intervals used is 42 for both the steady state and transient analyses. Values chosen for the crossflow resistance coefficient, the turbulent momentum factor, and transverse momentum factors are the representative of those used in subchannel analysis.

TABLE 2-1

INPUT PARAMETERS

Number of Axial Intervals	42
Crossflow Resistance Coefficient, k	0.5
Turbulent Momentum Factor, $f_t$	1.0
Transverse Momentum Factor, s/l	0.5
Flow Convergence Criterion*	0.01
Maximum Number of Hydraulic Iteration*	20

\*These are code default values



## SECTION 3

### HYDRAULIC MODEL DESCRIPTION

#### 3.1 Introduction

The techniques used in formulating the hydraulic model of Unit 1 of D. C. Cook Plant are, in general, applicable to all pressurized water reactors. The same techniques will be used in developing the hydraulic model for Unit 2. One-eighth core symmetry is assumed, and thus 1/8 core segment is modeled. It is also assumed that the hot assembly is located at the center of the core, and therefore, due to symmetry the 1/8 core segment contains 1/8 of the hot assembly. The hot assembly is modeled as an array of subchannels, while the remaining assemblies of the 1/8 core are modeled as lumped channels.

Using the above mentioned general techniques, a hydraulic model has been developed at AEP which is specifically applicable to Unit 1 of the Cook Plant. This model has 58 channels. Detailed description of this model along with a general description of Unit 1 core are provided in the following sections.

#### 3.2 General Description of the Cook Unit 1 Core

The Cook Unit No. 1 is the Westinghouse designed pressurized water reactor with core consisting of 193 fuel assemblies. The arrangement of the fuel assemblies is shown in Figure 3-1. Each fuel



assembly is hydraulically identical and consists of 204 fuel rods, 20 guide tubes, and a centrally located instrumentation tube. The fuel assembly array of 15 x 15 rods is shown in Figure 3-2. Hydraulic parameters of an assembly are listed in Table 3-1.

There are seven grids in each fuel assembly to support the fuel rods. These grids maintain the lateral spacings between fuel rods, and they are located at intervals along the assembly length. The five middle grids are called mixing vane grids since they contain tabs which project into the coolant stream. These grids are used in the high heat flux region to promote better mixing of the coolant. The internal straps of the two end grids do not contain mixing vanes, and therefore, they are called non-mixing vane grids. All grids are mechanically attached to the guide thimble tubes. The guide thimble tubes are in turn attached to the upper and lower nozzles and thus provide assembly structural support. Figure 3-3 shows the side view of the fuel assembly used in Unit 1 of the Cook Plant.

### 3.3 One-Eighth Core Representation

For steady state analysis of Unit 1 Core, a 58 channel model was developed representing an octant of the core. This 58 channel model consists of 30 lumped assembly channels and 28 subchannels. The radial geometries of the assembly and subchannel are depicted in Figures 3-4 and 3-5, respectively. In the axial direction, the seven grids are modeled by using grid loss coefficients at the axial positions listed in Table 3-2.

Each of the lumped assemblies, shown in Figure 3-4, were modeled using a lumped flow area, lumped heated and wetted perimeters, and an

effective gap. These hydraulic data, listed in Table 3-3, were calculated by considering the individual elements of the fuel assembly. The effective gap for crossflow is equal to the assembly pitch minus the blockage caused by the 15 fuel rods. Half assemblies formed by the lines of symmetry were modeled by multiplying the assembly hydraulic data by 0.5.

One-eighth of the central assembly was modeled in greater detail and is shown in Figure 3-5. It consists of four different types of subchannels. These are perimeter cell, corner cell, thimble cell and unit cell. The perimeter, corner and unit cells are all flow channels which are basically formed by four fuel rods. The perimeter and corner cells are modeled to include the flow region between the fuel rods of adjacent assemblies. The fourth type of subchannel is the thimble cell which is formed by three fuel rods and a guide/instrumentation thimble tube. Again, the half subchannels formed by the lines of symmetry were modeled by multiplying the subchannel hydraulic data by 0.5. The hydraulic data for all the four subchannels are given in Tables 3-4 through 3-7.

TABLE 3-1  
ASSEMBLY HYDRAULIC PARAMETERS

Number of Fuel Rods	204
Number of Guide Thimble Tubes	20
Number of Instrumentation Tubes	1
Fuel Rod Outside Diameter (in.)	0.422
Guide Thimble Tube Outside Diameter (in.)	0.545
Instrumentation Thimble Tube Outside Diameter (in.)	0.545
Fuel Rod Pitch (in.)	0.563
Fuel Assembly Pitch (in.)	8.466

TABLE 3-2

## AXIAL POSITIONS OF ASSEMBLY COMPONENTS

Description	Position (inches)
Start of Assembly	0.000
Start of Rodded Region	2.738
Start of Active Fuel	3.426
Non-mixing Vane Grid	5.263
Mixing Vane Grid	29.870
Mixing Vane Grid	56.060
Mixing Vane Grid	82.250
Mixing Vane Grid	108.440
Mixing Vane Grid	134.630
Non-mixing Vane Grid	153.590
End of Rodded Region	155.098
End of Assembly	156.285

TABLE 3-3 ASSEMBLY HYDRAULIC DATA

Fuel Assembly Flow Area (in. <sup>2</sup> )	38.24
Fuel Assembly Wetted Perimeter (in.)	306.41
Fuel Assembly Heated Perimeter (in.)	270.45
Fuel Assembly Effective Gap (in.)	2.136
Fuel Assembly Non-mixing Vane Grid Loss Coefficient	0.7378
Fuel Assembly Mixing Vane Grid Loss Coefficient	0.9182

TABLE 3-4 PERIMETER CELL HYDRAULIC DATA

Perimeter Cell Flow Area (in. <sup>2</sup> )	0.2716
Perimeter Cell Wetted Perimeter (in.)	1.989
Perimeter Cell Heated Perimeter (in.)	1.989
Fuel Rod to Fuel Rod Gap (in.)	0.141
Perimeter Cell Non-mixing Vane Grid Loss Coefficient	0.6732
Perimeter Cell Mixing Vane Grid Loss Coefficient	0.8377

TABLE 3-5 CORNER CELL HYDRAULIC DATA

Corner Cell Flow Area (in. <sup>2</sup> )	0.4163
Corner Cell Wetted Perimeter (in.)	2.983
Corner Cell Heated Perimeter (in.)	2.983
Fuel Rod to Fuel Rod Gap (in.)	0.141, 0.222*
Corner Cell Non-mixing Vane Grid Loss Coefficient	0.6732
Corner Cell Mixing Vane Grid Loss Coefficient	0.8377

TABLE 3-6 THIMBLE CELL HYDRAULIC DATA

Thimble Cell Flow Area (in. <sup>2</sup> )	0.1535
Thimble Cell Wetted Perimeter (in.)	1.423
Thimble Cell Heated Perimeter (in.)	0.994
Fuel Rod to Fuel Rod Gap (in.)	0.141
Fuel Rod to Guide Thimble Tube Gap (in.)	0.079
Thimble Cell Non-mixing Vane Grid Loss Coefficient	0.8953
Thimble Cell Mixing Vane Grid Loss Coefficient	1.114

\* Includes gap between the fuel rod and the grid strap.

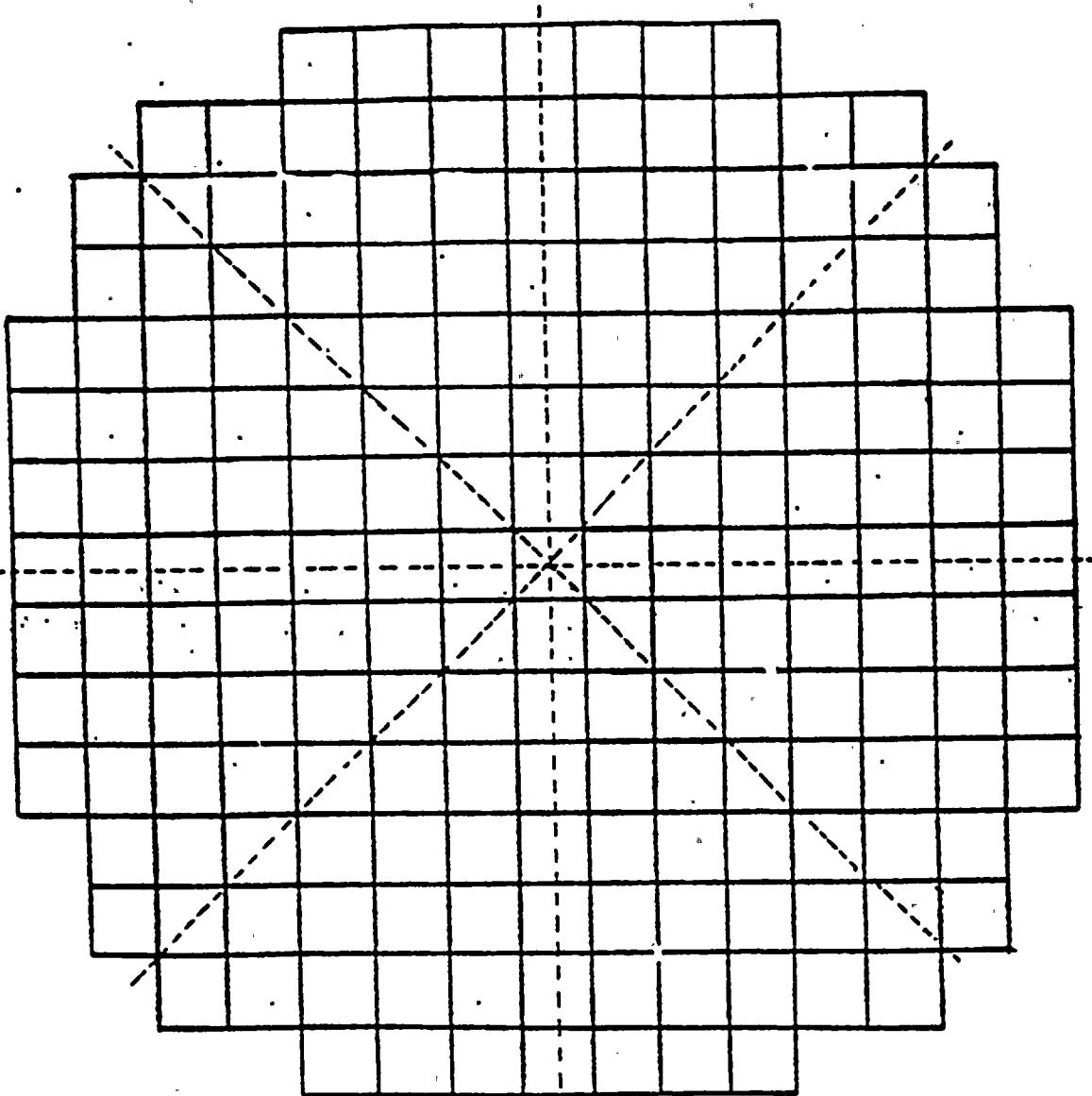
TABLE 3-7 UNIT CELL HYDRAULIC DATA

Unit Cell Flow Area (in. <sup>2</sup> )	0.1771
Unit Cell Wetted Perimeter (in.)	1.326
Unit Cell Heated Perimeter (in.)	1.326
Fuel Rod to Fuel Rod Gap (in.)	0.141
Unit Cell Non-mixing Vane Grid Loss Coefficient	0.6732
Unit Cell Mixing Vane Grid Loss Coefficient	0.8377

FIGURE 3-1

FUEL ASSEMBLY ARRANGEMENT OF

UNIT 1 OF DONALD C. COOK PLANT



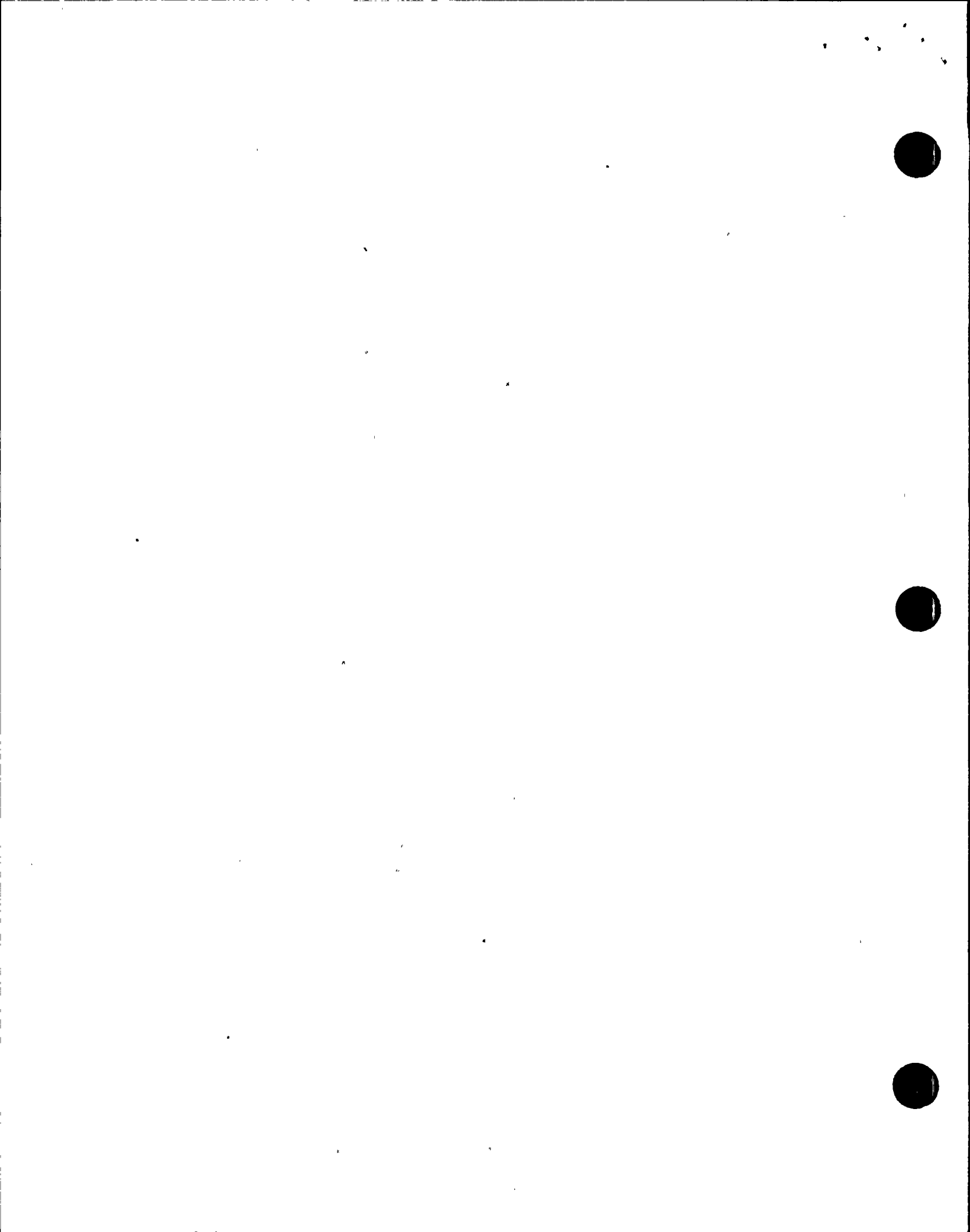


FIGURE 3-2

CROSS SECTIONAL VIEW OF COOK, UNIT 1 FUEL ASSEMBLY

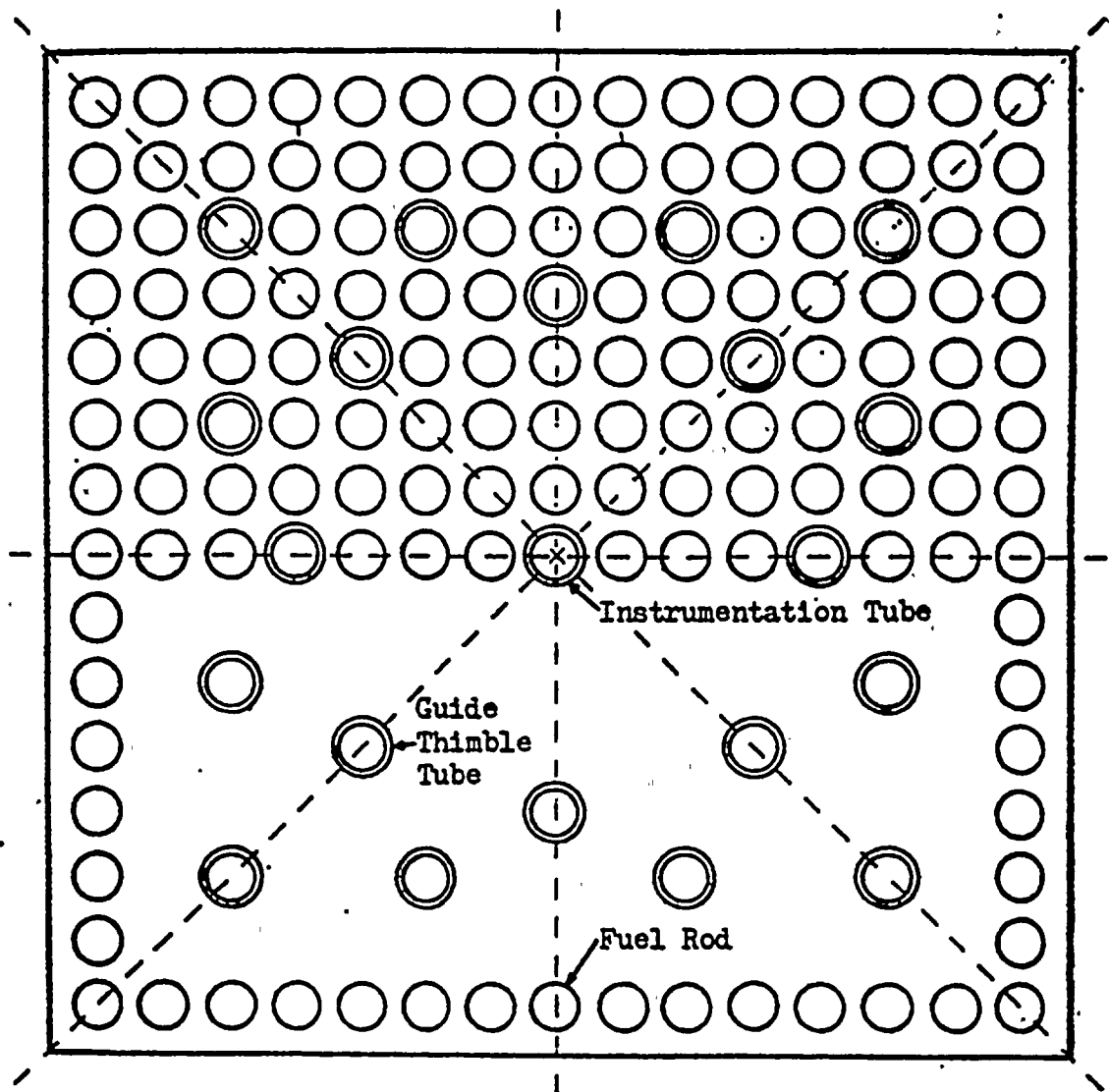
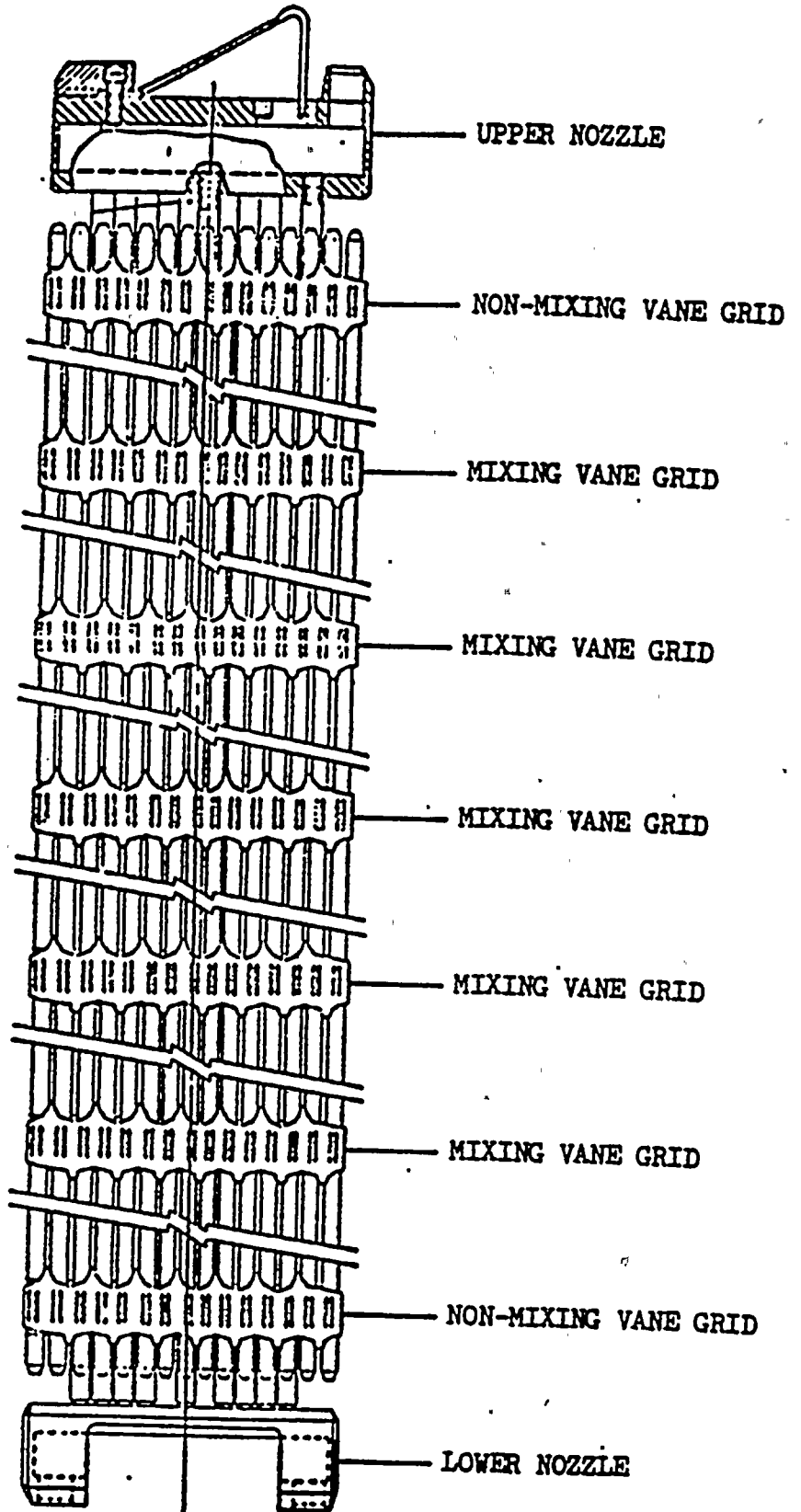


FIGURE 3-3

SIDE VIEW OF COOK, UNIT 1 FUEL ASSEMBLY



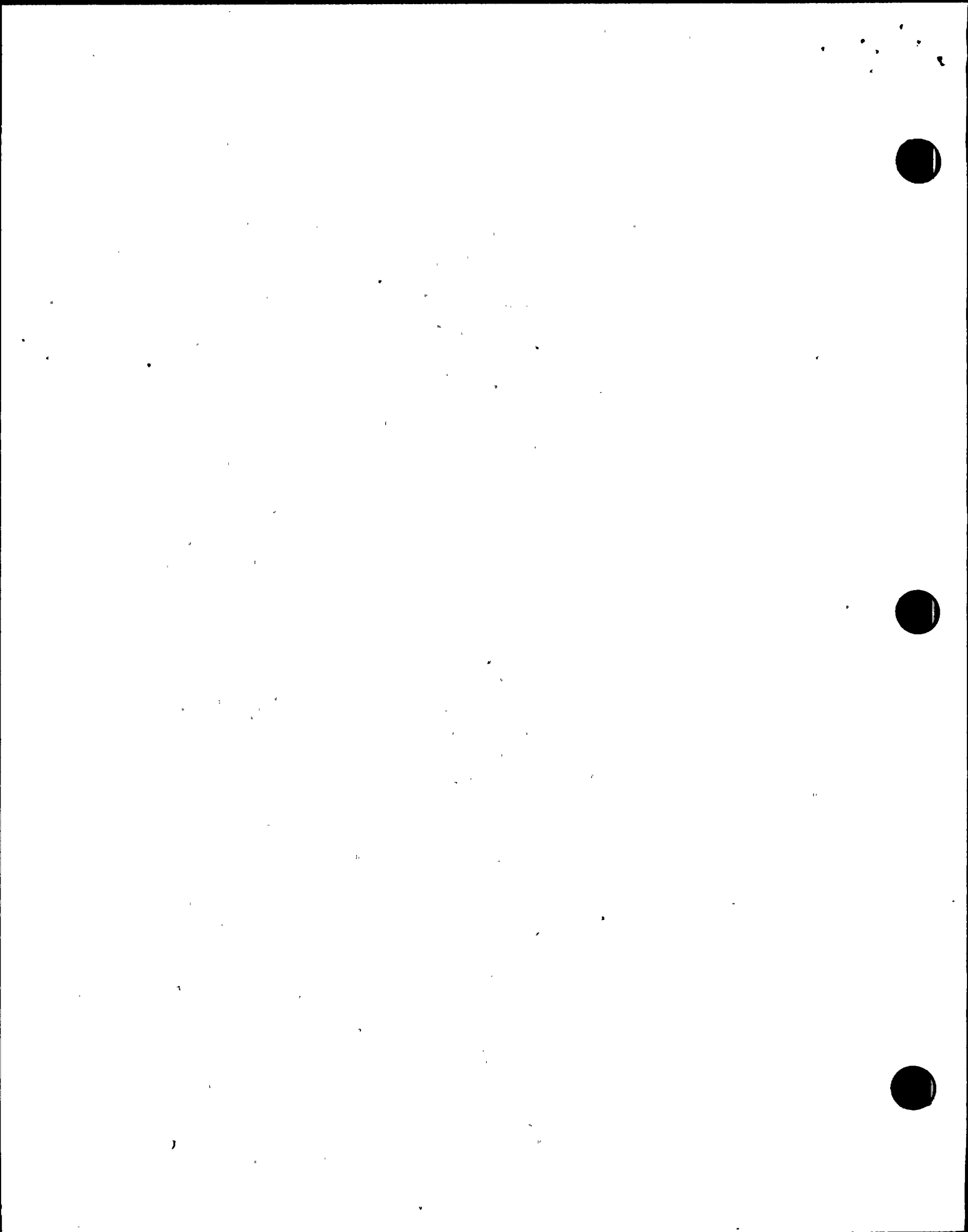


FIGURE 3-4

ONE-EIGHTH ASSEMBLY GEOMETRY OF 58 CHANNEL MODEL

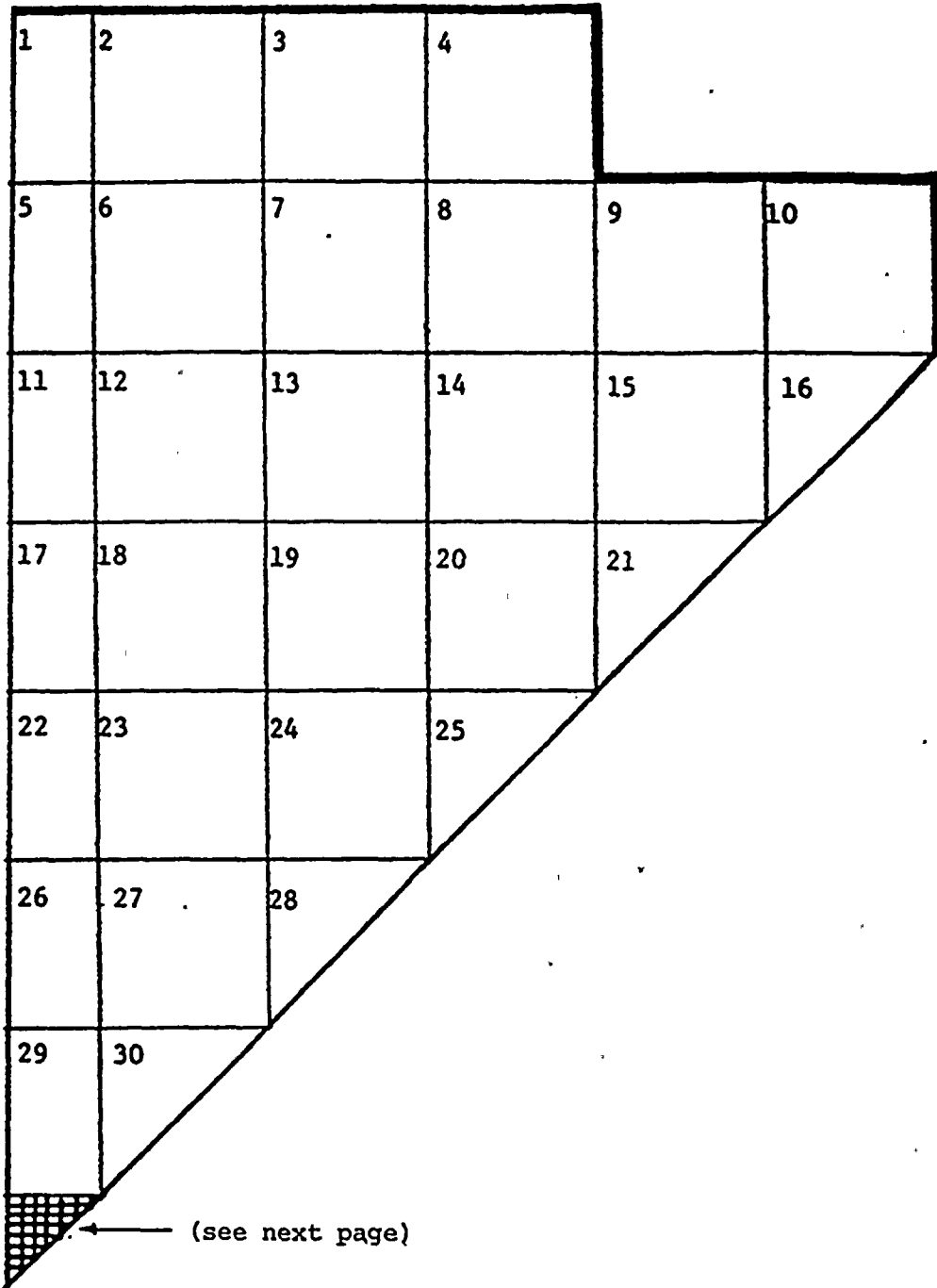
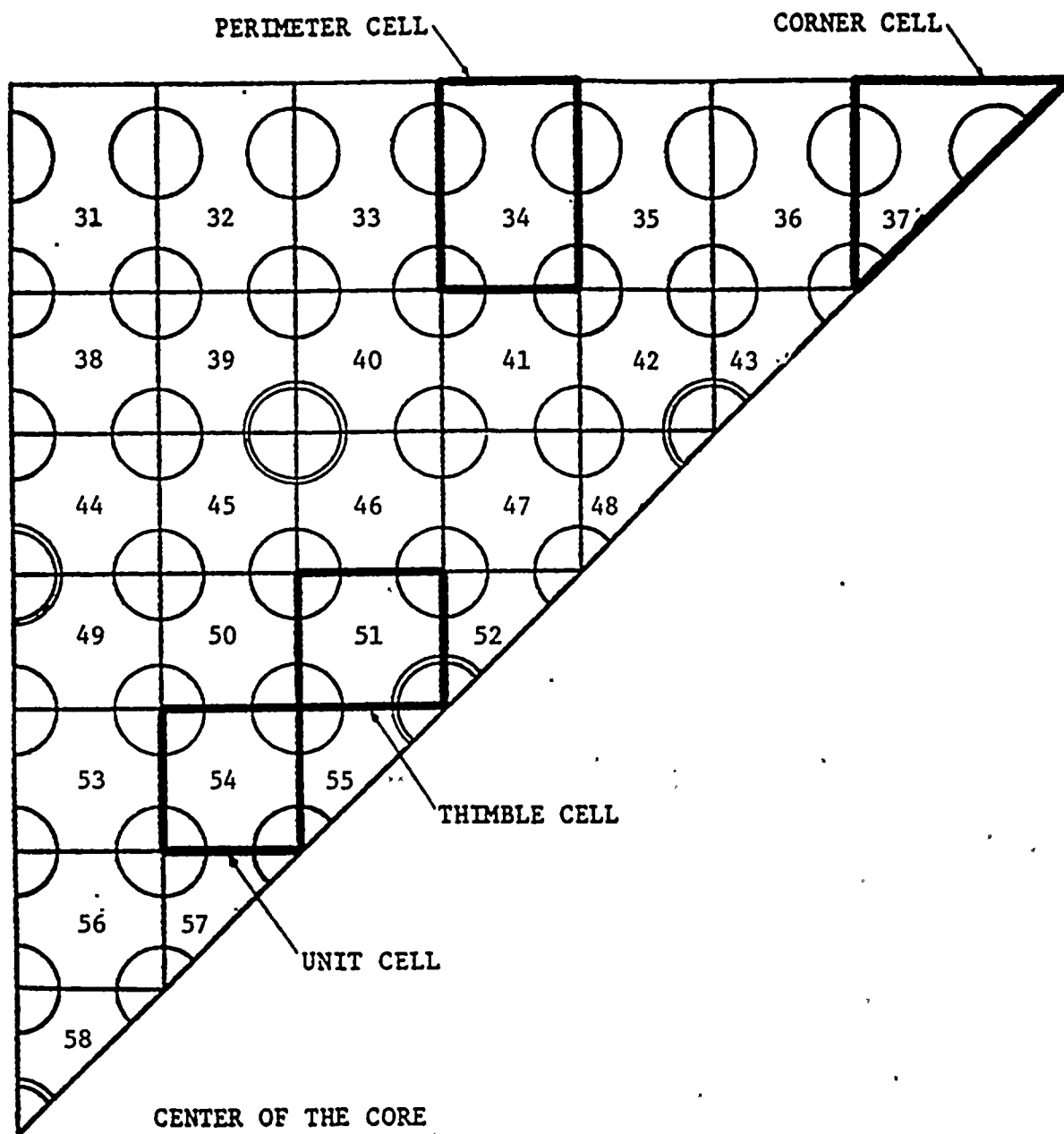




FIGURE 3-5

SUBCHANNEL GEOMETRY OF 58 CHANNEL MODEL



## SECTION 4

### THERMAL MODEL DESCRIPTION

#### 4.1 Introduction

The techniques used in developing the thermal model for D. C. Cook, Unit 1 core are applicable, in general, to all pressurized water reactors. The thermal model consists of an inlet flow distribution, radial and axial power distributions, and appropriate reactor operating conditions. For analyzing the transients, the time dependent forcing functions of system pressure, inlet flow, inlet temperature, and core power are also specified.

The thermal-hydraulic design parameters form the basis of this model. Thus the radial power distribution is based on the design value of  $F_{\Delta H}^N$ , and the axial power distribution is based on the axial flux shape. The core average mass velocity is calculated using the thermal design flow rate and core flow area. The core average heat flux is determined from power level and the heated area. The values for inlet temperature and system pressure are used as operating conditions.

In formulating the inlet flow distribution, the inlet flow to the hot assembly, i.e., the subchannel array, is conservatively reduced by 5% in order to account for the possibility of inlet flow maldistribution. In order to conserve the total flow rate, the

peripheral assemblies are given inlet flow fractions slightly greater than 1.0. The average of all the flow fractions is forced to equal 1.0.

In formulating the radial power distribution of the sub-channel portion, the fuel rods which form the hot channel are given relative power equal to the design value of  $F_{\Delta H}^N$  to maximize the heat flux to the hot channel. The relative powers to the remaining rods are so assigned that a gradual power gradient exists away from the hot channel. The average of all the fuel rod relative powers is forced to equal the hot assembly relative power. In general, power peaking within the hot assembly is assumed to be 5%, i.e., the ratio of  $F_{\Delta H}^N$  and the hot assembly relative power is 1.05.

In formulating the radial power distribution of the assembly portion, the hot assembly relative power is also assigned to the two assemblies adjacent to the subchannel array. Lower relative powers for the remaining assemblies are then assigned to create a second power gradient which peaks around the hot assembly. The average of all the assembly relative powers is forced to equal 1.0.

The above mentioned general techniques are used to formulate the D. C. Cook, Unit 1 thermal model. The thermal model is then imposed upon the hydraulic model to obtain the complete thermal-hydraulic model. Since this model is dependent on the thermal-hydraulic design parameters, therefore, this model must be revised to reflect any design changes. Generally, the hydraulic model relatively remains fixed since it is affected only by the changes in the mechanical design of the fuel. However, the thermal model can be significantly affected by changing any of the previously mentioned core design parameters.

#### 4.2 General Description of the Thermal Design of Cook, Unit 1 Core

The Unit No. 1 is a Westinghouse designed four loop pressurized water reactor with total power output of 3250 MWt. The following parameters are from Reference 4. The total flow rate is  $135.6 \times 10^6$  lbs/hr. The assumed flow effective for heat removal from the core is 95.5% (i.e., 4.5% bypass flow). The design nominal inlet temperature is  $536.3^\circ\text{F}$  and the nominal operating pressure is 2250 psia. The active fuel height is 143.4 inches, and the fraction of heat generated in the fuel is 0.974. In the original design of Unit 1, the values of nuclear enthalpy rise hot channel factor,  $F_{\Delta H}^N$  is 1.58 and that of nuclear heat flux hot channel factor,  $F_q^N$  is 2.71. These two values result in a maximum relative heat flux,  $F_z$  equal to 1.72.

#### 4.3 Inlet Flow Distribution

The inlet flow distribution used in 58 channel model is shown in Figure 4-1. This distribution was used in all the DNB analyses described within this report. Figure 4-1 shows that the hot assembly is given an inlet flow of 95%. The peripheral assemblies are given slightly higher fraction flow than 1.0. The average of all the flow fractions is approximately equal to 1.0.

#### 4.4 Radial Power Distribution

The radial power distribution for Cycle 1 formulated by AEP is shown in Figures 4-2 and 4-3. Figure 4-2 shows the radial power distribution for 1/8 of the core, while Figure 4-3 shows this distribution for 1/8 of the hot assembly. The centrally located hot assembly and two adjacent assemblies are given the radial power factor of 1.475. This value is the average of rod radial power factor of the hot assembly shown in Figure 4-3. The radial power factors for the remaining assemblies are assigned such that a power factor gradient exists around the hot assembly. The average of all the assembly relative powers is 1.0.

Figure 4-3 shows the radial power factor distribution for an octant of the hot assembly applicable to the 58 channel model. This power distribution has been used by VEPCO to develop their thermal-hydraulic methodology for the Surry Plant.<sup>(2)</sup> The use of this power distribution for Unit 1 is justified by the fact that the values of  $F_{\Delta H}^N$  and  $F_q^N$  used in Reference 2 are the same as for Cycle 1 of Cook Unit 1. Further, the fuel assemblies used in both cores were geometrically identical.

As shown in Figure 4-3, the hot channel is a thimble cell. Each of the three fuel rods surrounding the cell is given a relative power factor of 1.55, while the surrounding channels are assigned lower relative power factors such that a power gradient exists around the hot channel. The average of all the fuel rod relative powers is equal

to the hot assembly relative power of 1.475. Further, the ratio of peak to average rod power is 1.05.

#### 4.5 Axial Power Distribution

The generally used chopped cosine axial power distribution is not applicable to our DNB analysis, because such a profile is applicable for  $F_z \leq \pi/2$ . The reason for this is that the integral of a cosine profile with  $F_z > \pi/2$  does not yield a value of 1.0 when averaged over the active fuel height. An axial power distribution given by the following cosine function was used in our DNB analysis:

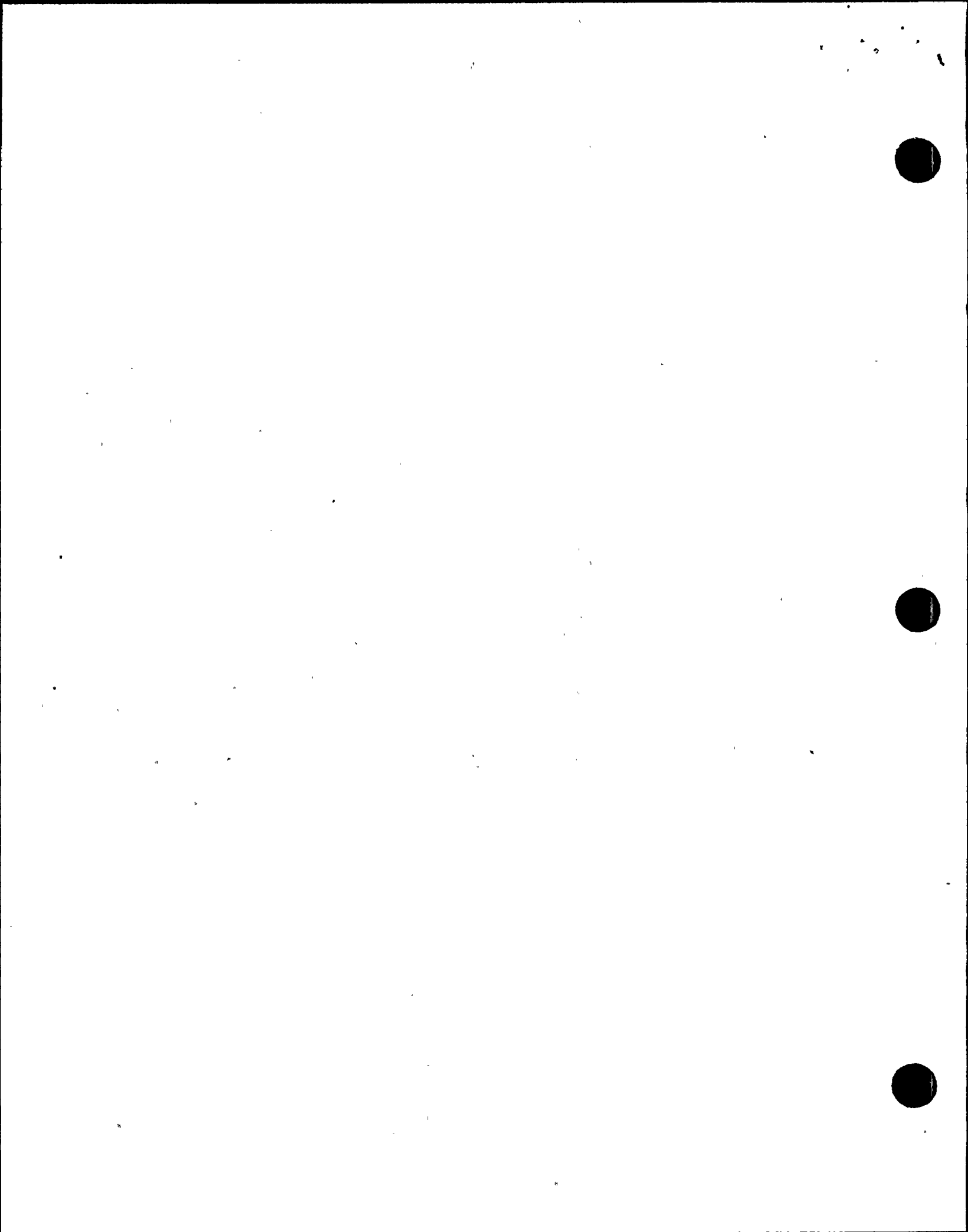
$$F(Z) = 1.72 \frac{[\cos \frac{\pi Z}{12}(1.56523) - \cos \frac{\pi}{2}(1.56523)]}{1 - \cos \frac{\pi}{2}(1.56523)}$$

where  $F(Z)$  = relative axial flux

$Z$  = distance from the core center, ft

The average of the above profile over the core height of 143.4 inches gives a value of 1.0.

For Unit 2, the value of  $F_z$  for the current cycle (Cycle 6) is 1.55<sup>(10)</sup>. For this case, the relative axial flux shape is 1.55 chopped cosine which is based on an active fuel length of 144 inches.



Values of relative flux as function of axial position are obtained using the following equation,

$$F(Z) = 1.55 \cos \frac{\pi Z}{H_e}$$

where  $H_e$  is the extrapolated length. In determining the extrapolated length,  $H_e$ , the integral of the above equation is averaged over the average length and set equal to 1.0. An iterative process is then used in order to determine the value of  $H_e$  which satisfies the resulting equation. For active core length of 144 inches, the value of  $H_e$  obtained is 12.164.

#### 4.6 Reactor Operating Conditions

The reactor operating conditions include core power level, core flow rate, core inlet temperature, and operating pressure. The Unit 1 is rated at a power level of 3250 MWt, the flow rate is  $135.6 \times 10^6$  lbs/hr, the design nominal inlet temperature is  $536.3^\circ\text{F}$ , and the operating pressure is 2250 psia. The operating conditions for the transient analysis are obtained by applying the maximum steady state errors to the rated values. The errors <sup>(11)</sup> used in minimum DNBR analysis are as follows:

Power	+2% over 3250 MWt
Temperature	+4°F over 536.3°F
Pressure	-30 psi over 2250 psia



#### 4.7 Forcing Functions for Transient Analysis

For performing the transient analysis, the COBRA IIIC/MIT-2 computer code requires the four normalized forcing functions, namely, pressure versus time, enthalpy or inlet temperature versus time, average mass flow versus time, and channel power versus time. These forcing functions were obtained from Unit 1 FSAR and normalized by their initial values. These forcing functions can also be obtained from transient analysis performed using thermal hydraulic systems code, such as RELAP5. The COBRA code requires these functions to be input in the form of tables.

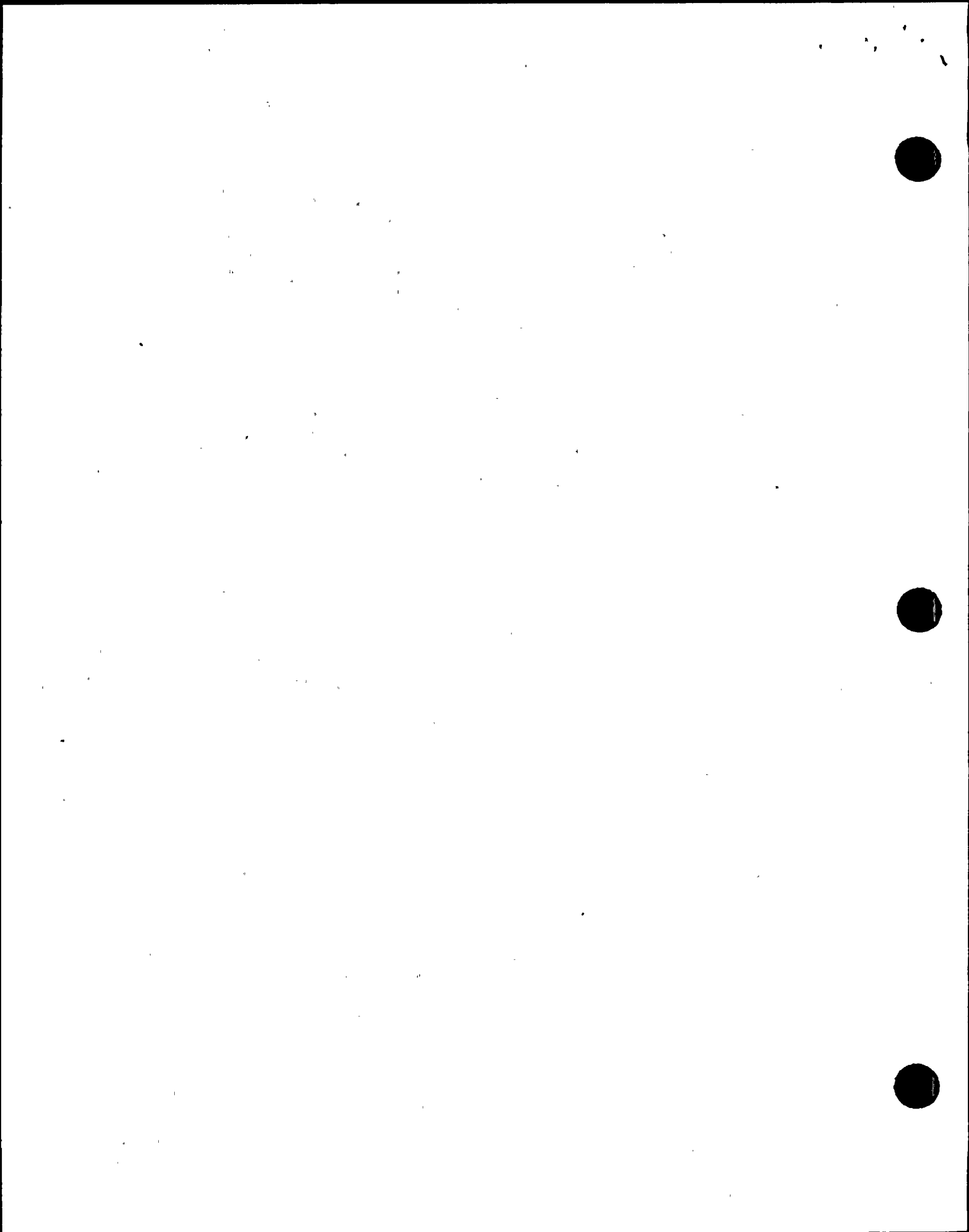




Figure 4-2

ASSEMBLY POWER DISTRIBUTION OF 58 CHANNEL MODEL

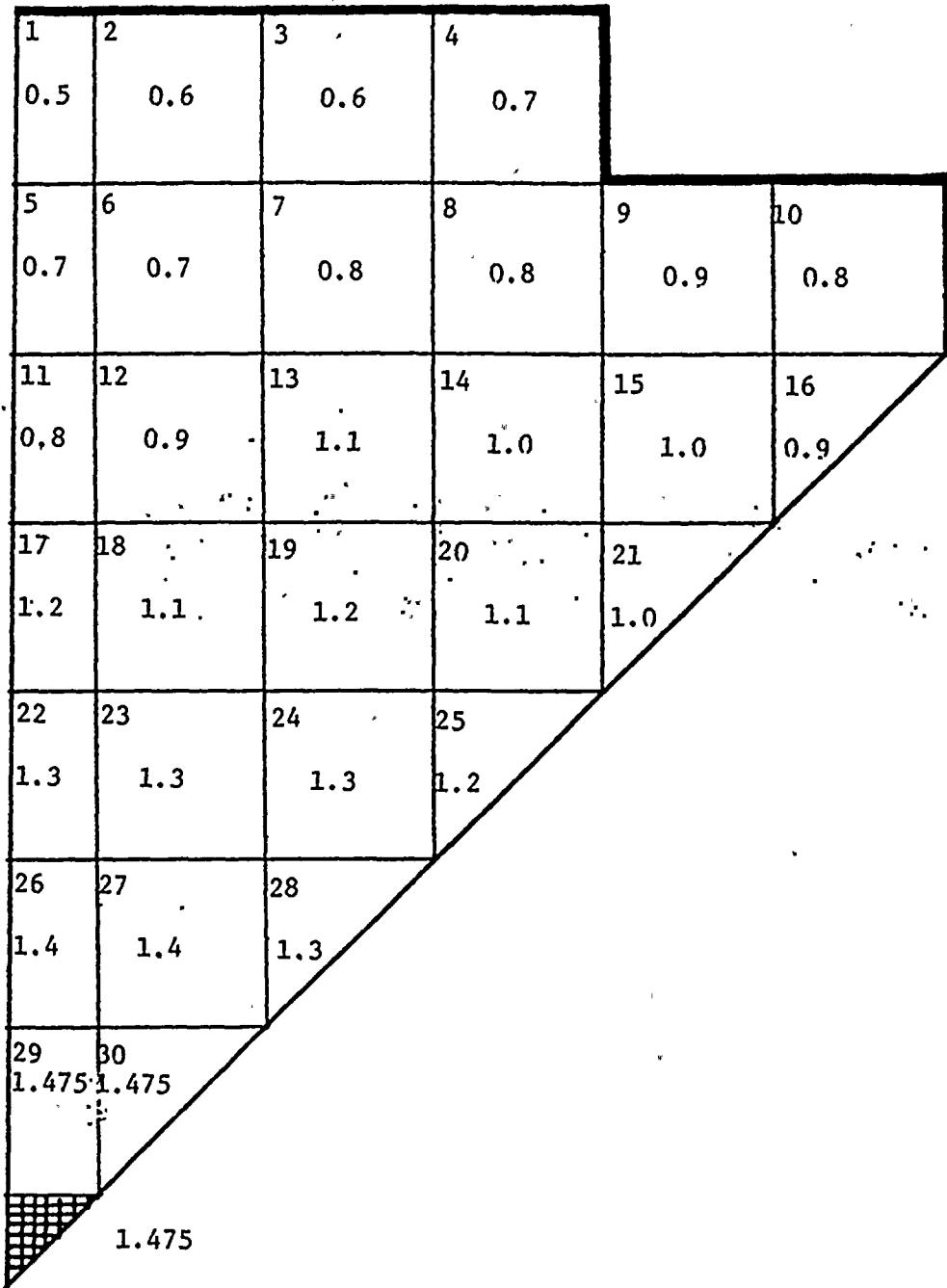
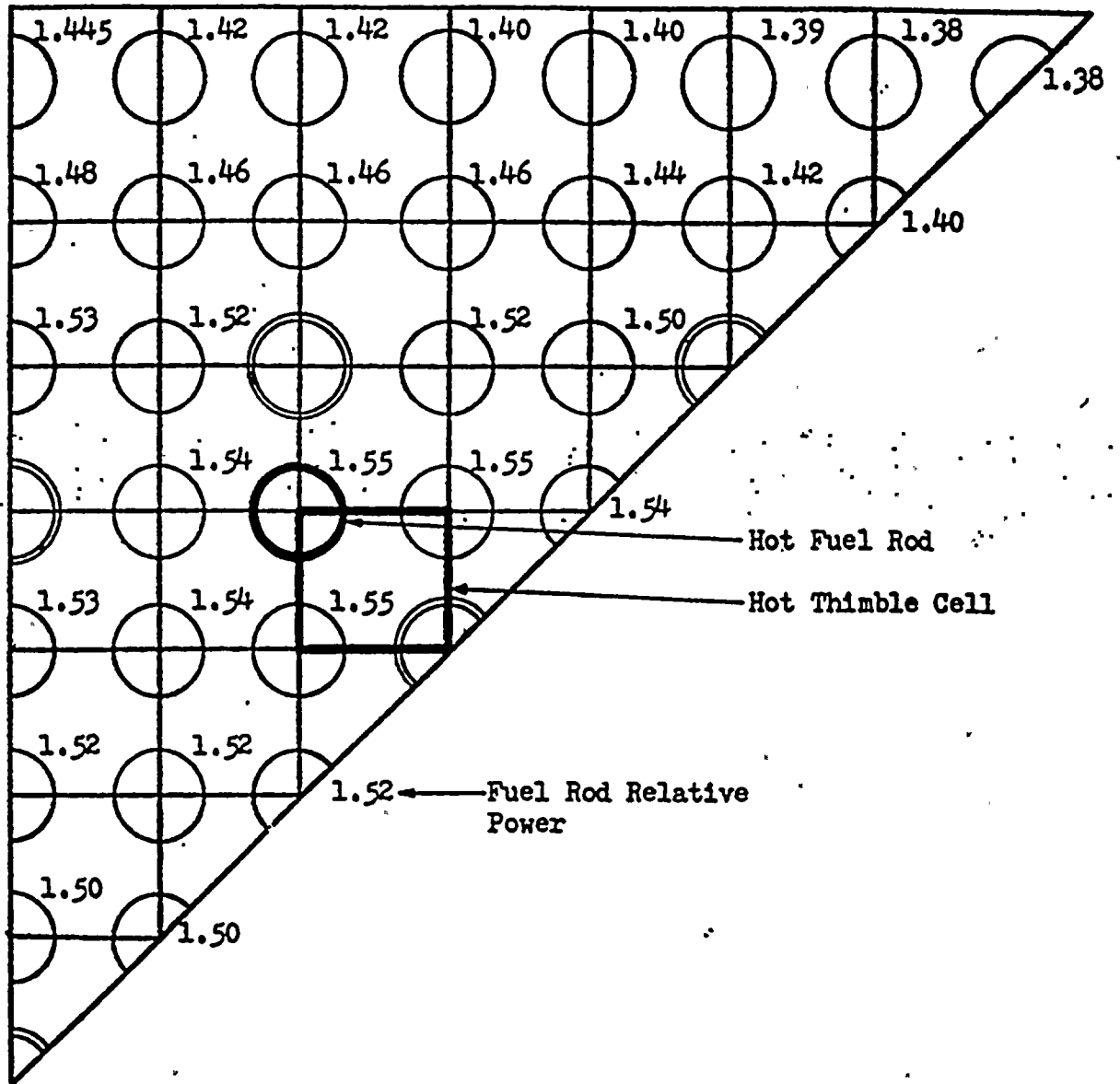
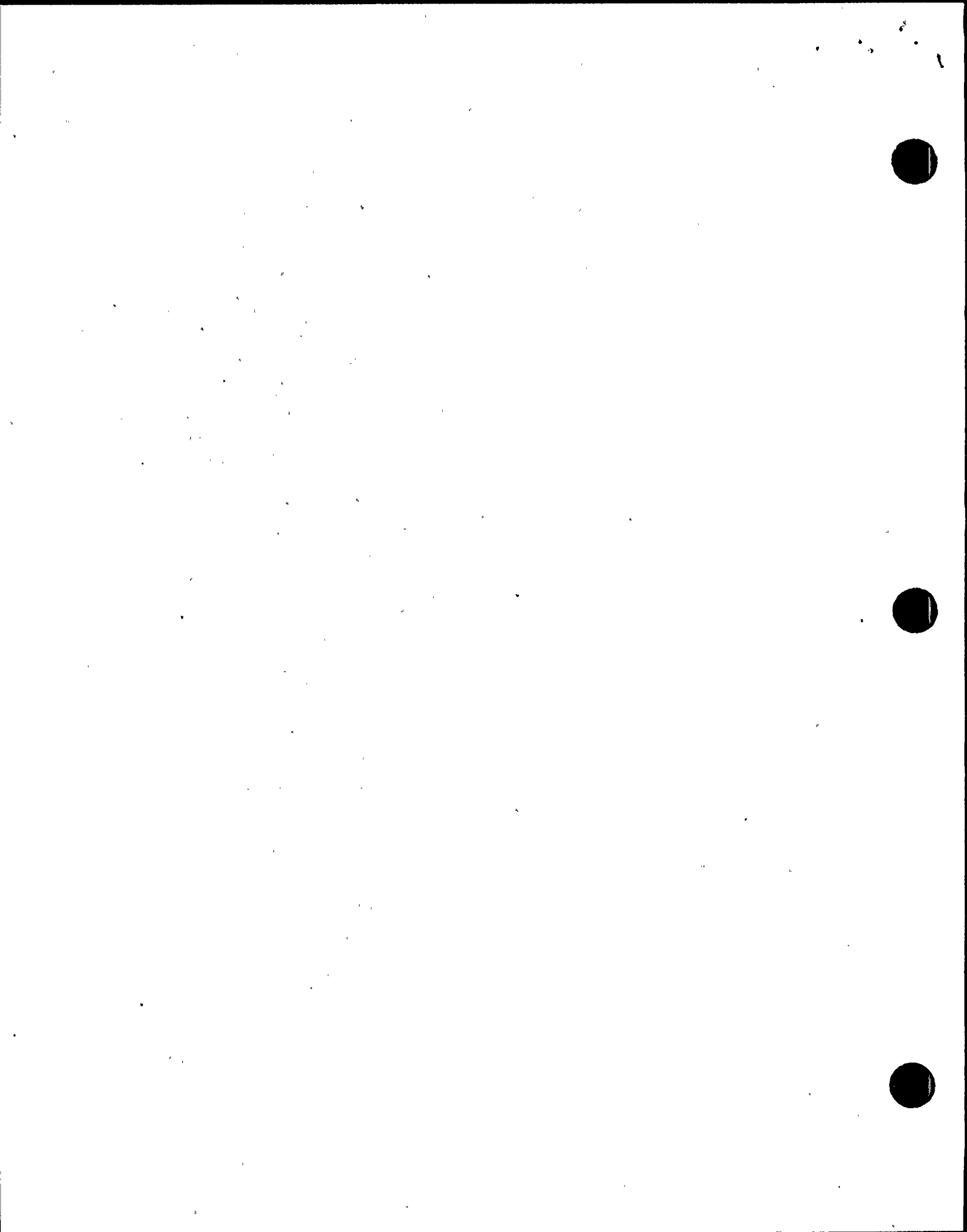




Figure 4-3

SUBCHANNEL POWER DISTRIBUTION OF 58 CHANNEL MODEL





## SECTION 5

### ENGINEERING UNCERTAINTIES

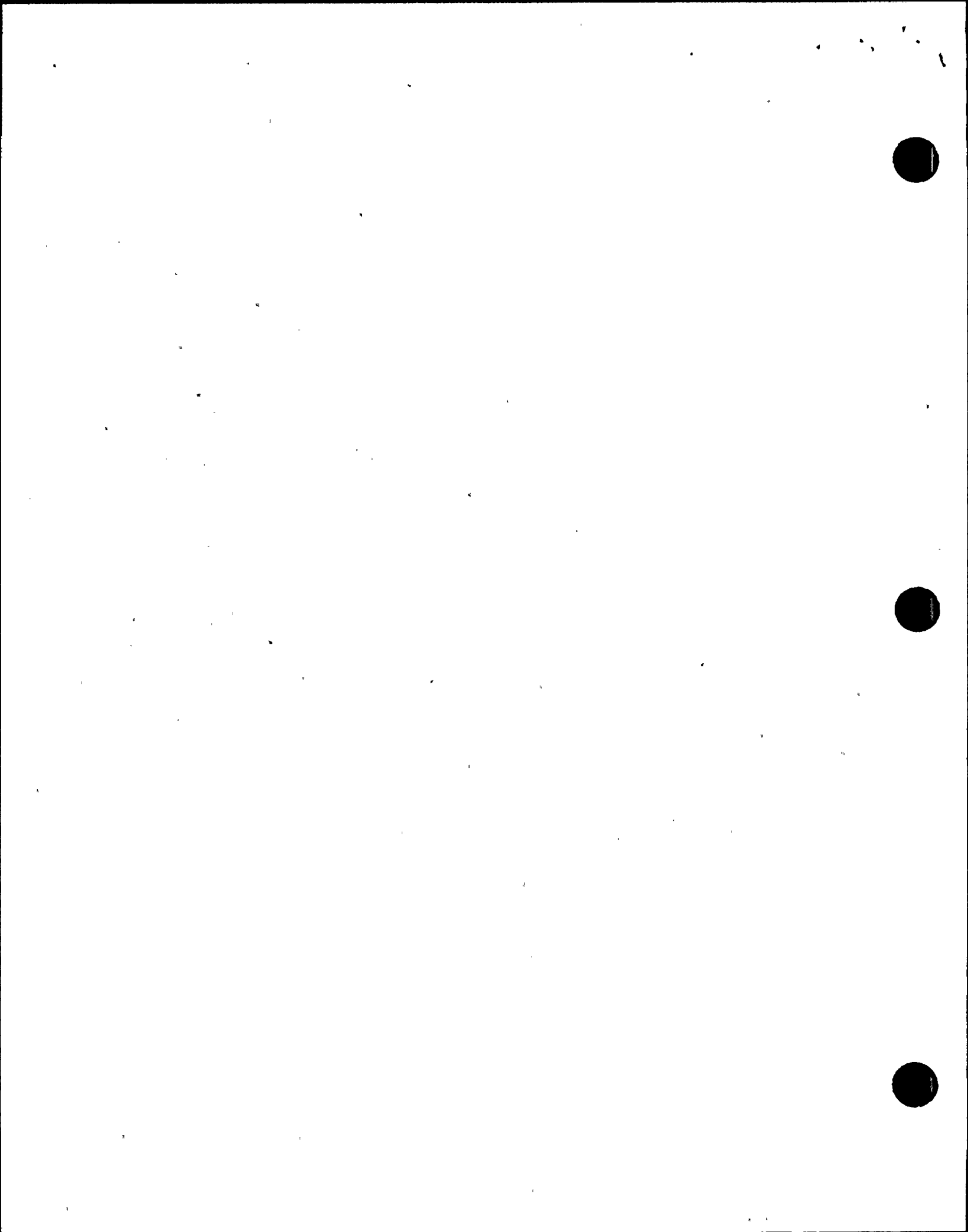
#### 5.1 Introduction

The hydraulic and thermal models for Cook, Unit 1, Cycle 1 are described in Sections 3 and 4, respectively. These two models are combined to formulate the overall thermal-hydraulic representation of the core. Engineering uncertainties are applied to this model in order to account for the effects of flow conditions and manufacturing tolerances used in fuel fabrication. It is assumed that the fabrication tolerances occur in the hot channel, and they are therefore called the hot channel factors. The following sections briefly describe these factors and their application in DNB analysis.

#### 5.2 Heat Flux Engineering Subfactor, $F_q^E$

This subfactor is defined as a ratio of local maximum at a point to core average heat flux. The  $F_q^E$ , used to evaluate the maximum heat flux, is determined by statistically combining the tolerances for the fuel diameter, density, enrichment and fuel rod diameter, pitch and bowing. The value of  $F_q^E$  is 1.03 (Reference 4).

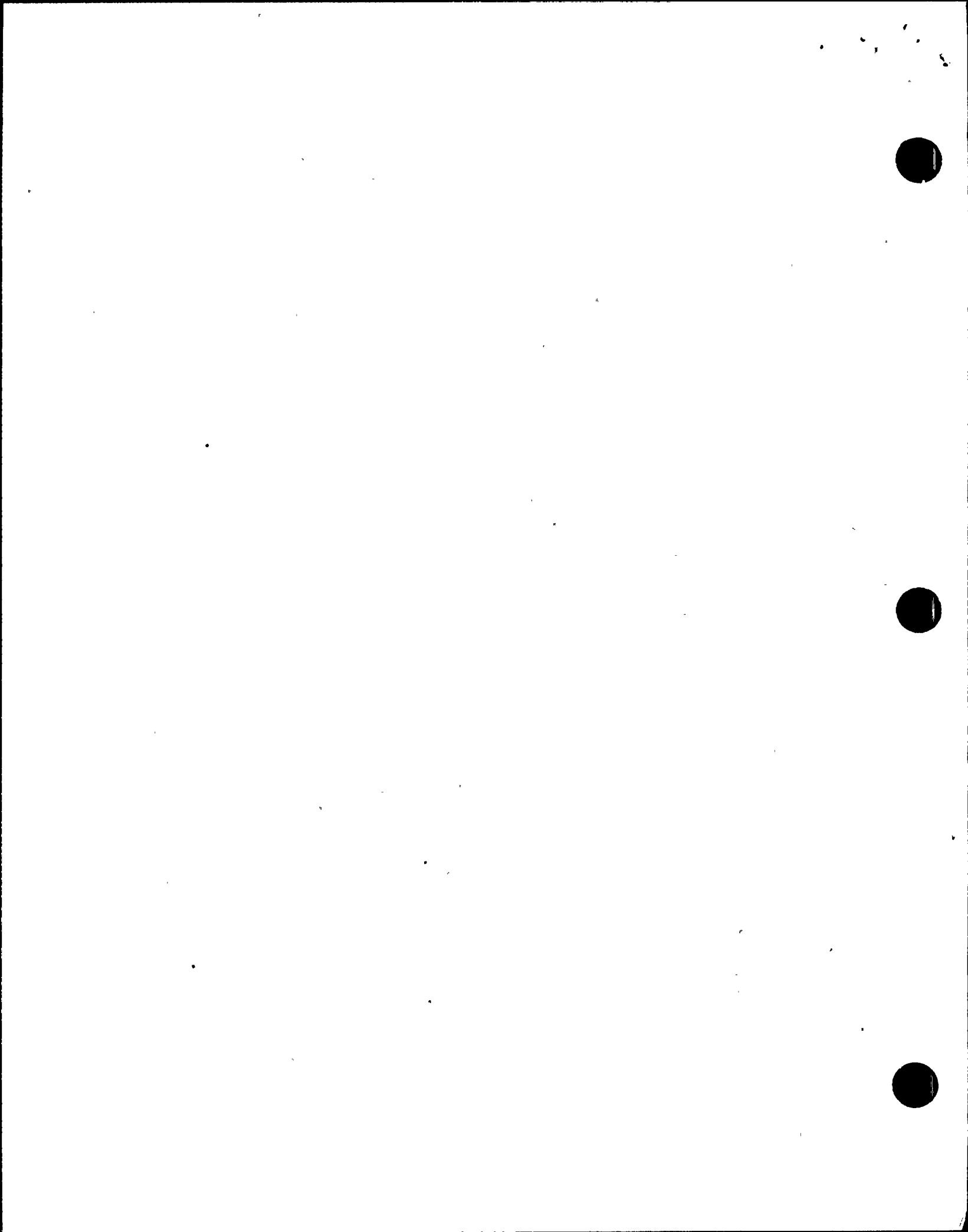
The  $F_q^E$  is accounted for by applying a heat flux spike on the hot fuel rod at the position of MDNBR. Before the heat flux spike can be applied, however, a thermal analysis must be performed in order to determine the axial position of MDNBR. The axial heat flux shape for the hot fuel rod is then adjusted to include the heat flux spike at the determined position. This axial flux shape is then used to obtain the final value of MDNBR.



It should be noted that recent spike DNB tests have shown that the actual spike effect on DNB is very small.<sup>(12)</sup> Based on these results, it was concluded that  $F_q^E$  need not be considered in DNB evaluation since its effect could be adequately accounted for in the DNBR design limit.

### 5.3 Enthalpy Rise Engineering Subfactor, $F_{\Delta H}^E$

This subfactor is defined as a ratio of maximum to core average enthalpy rise along a channel. The  $F_{\Delta H}^E$  is built-up of various subfactors.<sup>(13)</sup> These are pellet diameter, density enrichment and fuel diameter, pitch and bowing (1.08); inlet flow maldistribution (1.01); flow redistribution (1.03), and flow mixing (0.90). The resulting  $F_{\Delta H}^E$  is 1.01. For all the DNB analyses described within this report, the relative power of the hot fuel rod was multiplied by a factor of 1.02.



## SECTION 6

### THERMAL-HYDRAULIC MODEL VERIFICATION

#### 6.1 Introduction

The thermal-hydraulic model developed by AEP was described in the preceding sections. This model was tested to verify its accuracy. Three steady state and three transient DNB analyses were performed using AEP methodology. These analyses are listed in Table 6-1.

The analyses performed were simulated as closely as possible to the original analyses. Verification was performed by comparing the results obtained by AEP methods with those given in the original analysis/licensing documents. The details of these analyses and results are given in the following subsections.

#### 6.2 Steady State Analysis

Three steady state analyses performed were selected from different sources to verify the calculational accuracy of the AEP methods. The COBRA IIIC/MIT-2 code input was developed for each of these cases by using the reactor core data provided in original analysis/documents. These analyses are described briefly below:

##### 6.2.1 Surry Core Analysis at 100% Power Performed by VEPCO

The Virginia Electric and Power Company has performed the Surry core analysis <sup>(2)</sup> for developing their thermal-hydraulic methodology. A 53 channel model was used in this analysis. The reactor core data used by VEPCO in their model formulation are listed in Tables 6-2 and 6-3. The radial power distribution for 1/8 of core and 1/8 of hot assembly are shown in Figures 6-1 and 6-2. Using AEP methods, a MDNBR of 1.90 was calculated.

This result is in excellent agreement with the value of 1.94 obtained by VEPCO. (2)

#### 6.2.2 Three-Loop Westinghouse PWR Analysis at 118%

##### Power Performed by ANF

Advanced Nuclear Fuels Company (ANF) has performed the hot channel calculations for overpower steady-state conditions for a 3-loop Westinghouse PWR containing 15x15 array fuel assemblies. (3) The hot channel calculations were made using their XCOBRA-IIIC computer code. A 36 subchannel model representing the 1/8 of hot assembly was used in this analysis. The core operating data used are listed in Table 6-4. The value of MDNBR obtained using AEP methodology is 1.86 which compares well with 1.985 obtained by ANF.

#### 6.2.3 Cook, Unit 1 FSAR Analysis at 100% Power

The steady state analysis for Cook, Unit 1 was made using thermal-hydraulic data from original FSAR (13) and listed in Table 6-5. The assembly power distribution used for 1/8 of core is shown in Figure 6-3. The radial power distribution used for 1/8 of hot assembly is same as for Surry core and shown in Figure 6-2. Table 6-6 contains the axial flux distribution used in the present case. The MDNBR obtained using AEP methodology is 1.93. This result is in excellent agreement with the FSAR value of 1.97.

### 6.3 Transient Analysis

Three transients used for AEP methods verification are listed in Table 6-1. These transients are the same as used by VEPCO for their thermal-hydraulic methodology verification. The operating conditions of these transients were obtained from original FSAR <sup>13</sup>. The analyses performed and results obtained are described briefly in the following subsections:

#### 6.3.1 Excessive Load Increase Transient

An excessive load increase transient results from a rapid increase in steam generator steam flow causing a power mismatch between the reactor core power and steam generator load demand. This transient could be caused from either an administrative violation, such as excessive loading by the operator or an equipment malfunction in the steam dump control or turbine speed control.

The reactor control system is designed to accommodate a 10% step load increase without a reactor trip. Analyses are performed to demonstrate that MDNBR does not fall below the design limit for such cases. The case analyzed is a 10% step increase at EOL with reactor at full power under manual control. The initial operating conditions used are described in Section 4.6. The forcing functions of core power, system pressure, and inlet temperature were obtained from Cook, Unit 1 FSAR. The DNBR results obtained using AEP methodology are shown in Figure 6-4. The MDNBR obtained for this transient is 1.57 while the FSAR value is 1.56.



### 6.3.2 Uncontrolled Control Rod Assembly Withdrawal at Power Transient

An uncontrolled RCC assembly withdrawal at power transient results in an increase in core heat flux. Since the heat extraction from the steam generator lags behind the power generation until the steam generator pressure reaches the relief or safety valve setpoint, there is a net increase in reactor coolant temperature.

Unless terminated by manual or automatic action, the power mismatch and resultant coolant temperature rise would eventually result in DNB. The case analyzed is a slow control rod assembly withdrawal (reactivity insertion rate  $- 2.0 \times 10^{-5}$  k/sec) from full power. The forcing functions of core power, system pressure, and inlet temperature were obtained from Cook, Unit 1 FSAR.

DNBR results obtained using AEP methodology are shown in Fig. 6-5. The MDNBR obtained is 1.42 while the FSAR value is 1.40.

### 6.3.3 Complete Loss of Reactor Coolant Flow Transient

A complete loss of coolant flow transient can result from a simultaneous loss of electric supplies to all the four reactor coolant pumps. If the reactor is at power at the time of incident, the immediate effect of loss of coolant flow is a rapid increase in the coolant temperature. This increase could result in DNB with subsequent fuel damage if the reactor is not tripped promptly. The case analyzed is a complete loss of reactor



coolant flow from 100% power. The reactor is assumed to be tripped on undervoltage signal and the time from initiation of the incident to initiation of control rod motion is assumed to be 1.2 sec. The forcing functions of core average heat flux and core flow were obtained from Cook, Unit 1 FSAR.

System pressure and inlet temperature were assumed constant throughout the transient. DNBR results obtained using AEP methodology are shown in Figure 6-6. The MDNBR obtained for this transient is 1.38 while the FSAR value is 1.40.

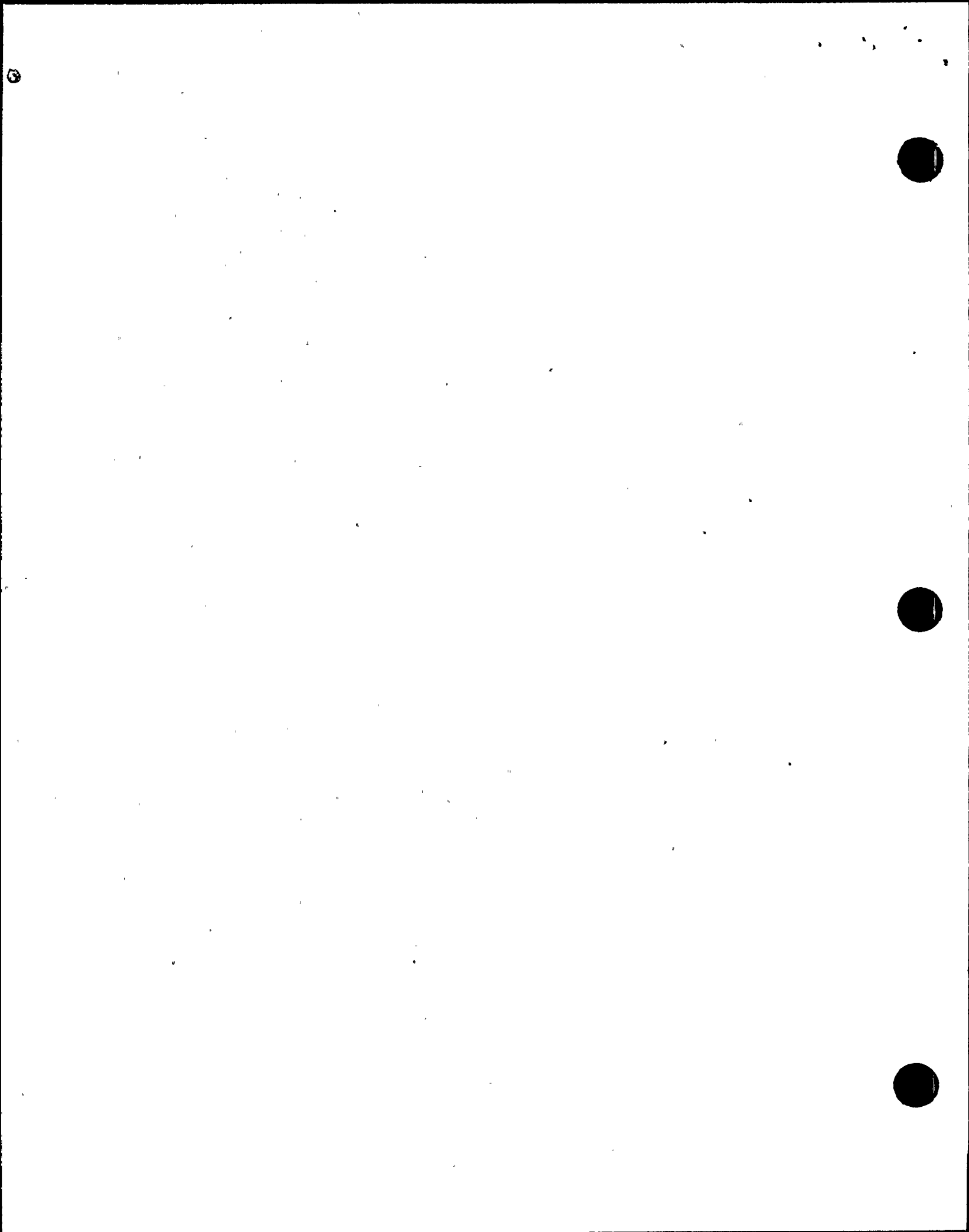


TABLE 6-1

LISTING OF AEP VERIFICATION ANALYSES

Steady State Analyses

1. Surry Core Analysis at 100% Power Performed by VEPCO
2. Three-Loop Westinghouse PWR Analysis at 118% Power Performed by ANF
3. Cook, Unit 1 FSAR Analysis at 100% Power

FSAR Transient Analyses (Cook Unit 1, Cycle 1)

1. Excessive Load Increase Transient
2. Uncontrolled Control Rod Assembly Withdrawal at Power Transient
3. Complete Loss of Reactor Coolant Flow Transient

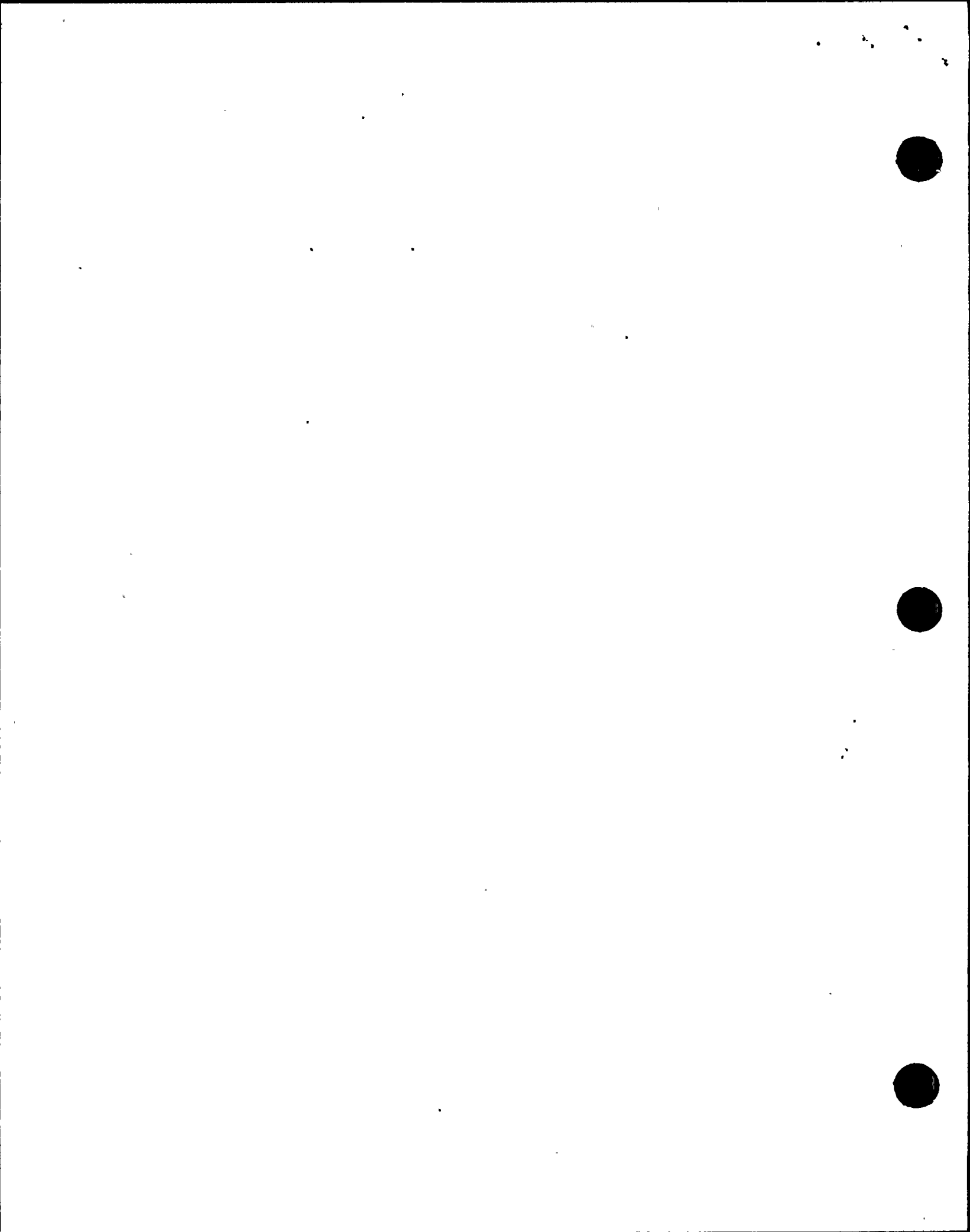


TABLE 6-2

## REACTOR CONDITIONS FOR SURRY CORE ANALYSIS

Power (% of nominal 2441 MWt)	100
Core Average Heat Flux, $10^6$ Btu/hr-ft <sup>2</sup>	0.196206
Inlet Temperature, °F	543
System Pressure, psia	2250
Core Average Mass Velocity, $10^6$ lbm/hr-ft <sup>2</sup>	2.308
$F_{\Delta H}$ (Hot Unit Cell)	1.58
$F_Z$	1.72
Hot Assembly Relative Power	1.432
Active Fuel Length (inches)	144.0
Reactor flow, gpm at 543 °F	265,500
$F_q^E$	1.03
$F_{\Delta H}^E$	1.02
CHF Correlation	W-3 with F-Factor

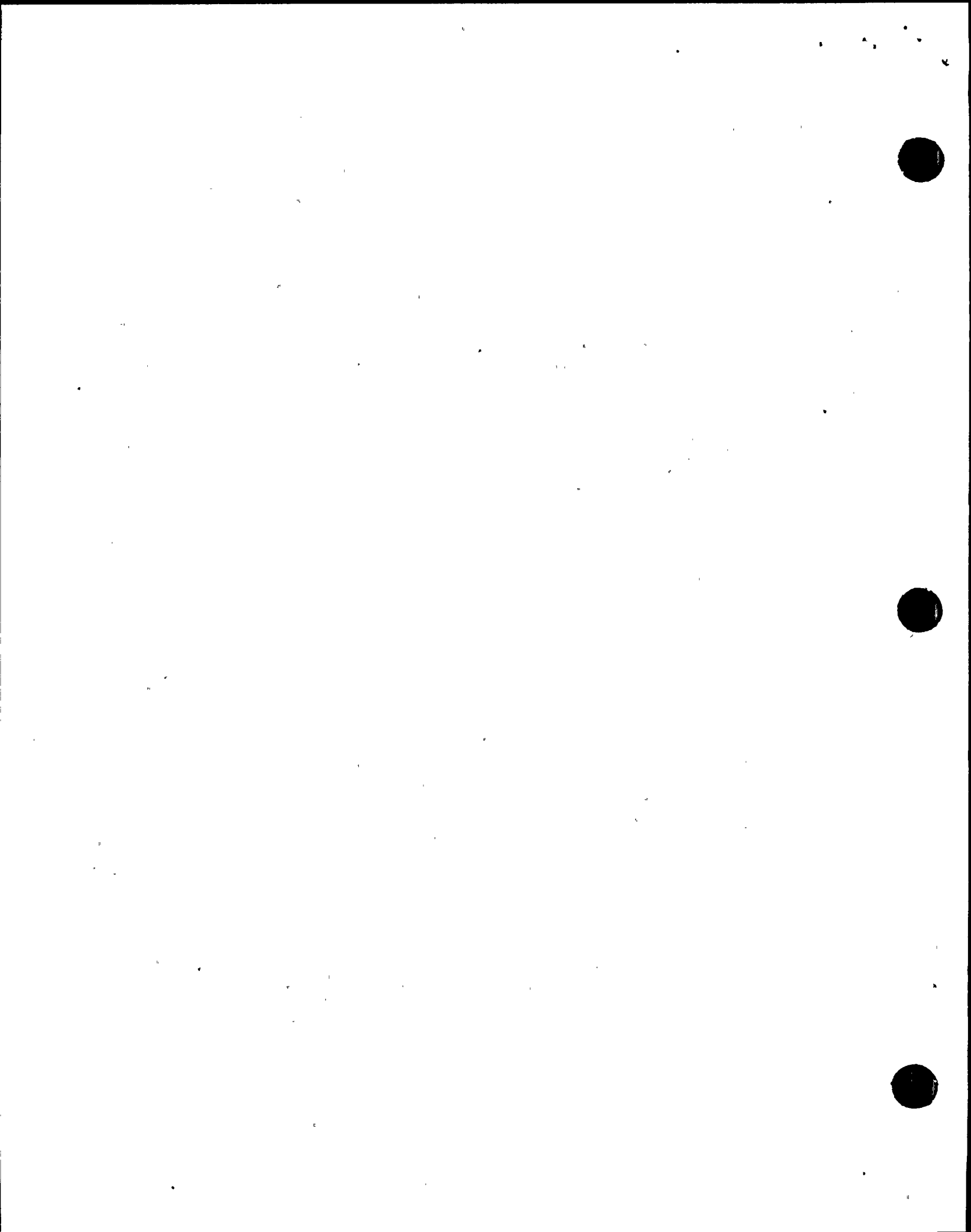


TABLE 6-3

AXIAL POWER DISTRIBUTION FOR SURRY CORE ANALYSIS

$$F(z') = 1.72 \frac{\cos \frac{\pi z' (1.56523)}{12} - \cos \frac{\pi (1.56523)}{2}}{1 - \cos \frac{\pi (1.56523)}{2}}$$

Axial Flux Shape: 1.72 Cosine (144.0" Active Length)

<u>z/156.0</u> <u>Relative Position</u>	<u>F(z')</u> <u>Relative Flux</u>
0.0000	0.0000
0.0192	0.0000
0.0654	0.1714
0.1115	0.3776
0.1577	0.6064
0.2038	0.8438
0.2500	1.0757
0.2962	1.2881
0.3423	1.4682
0.3885	1.6052
0.4346	1.6909
0.4808	1.7200
0.5269	1.6909
0.5731	1.6052
0.6192	1.4682
0.6654	1.2881
0.7115	1.0757
0.7577	0.8438
0.8038	0.6064
0.8500	0.3776
0.8962	0.1714
0.9423	0.0000
1.0000	0.0000



TABLE 6-4

REACTOR CONDITIONS FOR 3-LOOP WESTINGHOUSE  
PWR ANALYSIS

Overpower Steady-State Condition

Power (118% of rated power), MWt	2714
Operating Pressure, psia	2250
Coolant Inlet Temperature, °F	547
Core Average Mass Velocity, $10^6$ lbm/hr-ft <sup>2</sup>	2.342
Fraction of Heat Generated in Fuel	0.974
Active Fuel Length, inches	144.0

Hot Assembly Conditions

Power (118% of rated power), MWt	24.63
Average LHGR, kw/ft	9.80
Average Mass Velocity, $10^6$ lbm/hr-ft <sup>2</sup>	2.315

Hot Channel Factors

$F_q^N$	2.40
$F_{\Delta H}^N$	1.55
$F_Z$	1.55
Hot Assembly Relative Power	1.425
$F_q^E$	1.02
Total Enthalpy Rise Factor $F_{\Delta H}$	1.59
CHF Correlation	W-3

TABLE 6-5

REACTOR CONDITIONS FOR COOK, UNIT 1  
FSAR STEADY STATE ANALYSIS

Power (% of nominal 3250 MWt)	100
Core Average Heat Flux, $10^6$ Btu/hr-ft <sup>2</sup>	0.2124
Inlet Temperature, °F	536.3
System Pressure, psia	2250
Core Average Mass Velocity, $10^6$ lbm/hr-ft <sup>2</sup>	2.53
(This is 95.5% of total flow rate)	
$F_{\Delta H}$ (Hot Unit Cell)	1.58
$F_Z$	1.72
Hot Assembly Relative Power	1.432
Active Fuel Length, inches	143.4
Total Flow rate, $10^6$ lbm/hr	135.6
$F_q^E$	1.03
$F_{\Delta H}^E$	1.02
CHF Correlation	W-3 with F-Factors

TABLE 6-6

AXIAL POWER DISTRIBUTION FOR COOK, CORE ANALYSIS

$$F(z') = 1.72 \frac{\cos \frac{\pi z' (1.56523)}{12} - \cos \frac{\pi (1.56523)}{2}}{1 - \cos \frac{\pi (1.56523)}{2}}$$

Axial Flux Shape: 1.72 Cosine (143.4" Active Length)

<u>Z/156.3</u> <u>Relative Position</u>	<u>F(Z')</u> <u>Relative Flux</u>
0.0000	0.0000
0.0219	0.0000
0.0678	0.1714
0.1137	0.3776
0.1596	0.6064
0.2054	0.8438
0.2513	1.0760
0.2972	1.2880
0.3431	1.4680
0.3889	1.6050
0.4348	1.6910
0.4807	1.7200
0.5266	1.6910
0.5725	1.6065
0.6183	1.4680
0.6642	1.2880
0.7101	1.0760
0.7560	0.8438
0.8018	0.6064
0.8477	0.3776
0.8936	0.1714
0.9395	0.0000
1.0000	0.0000

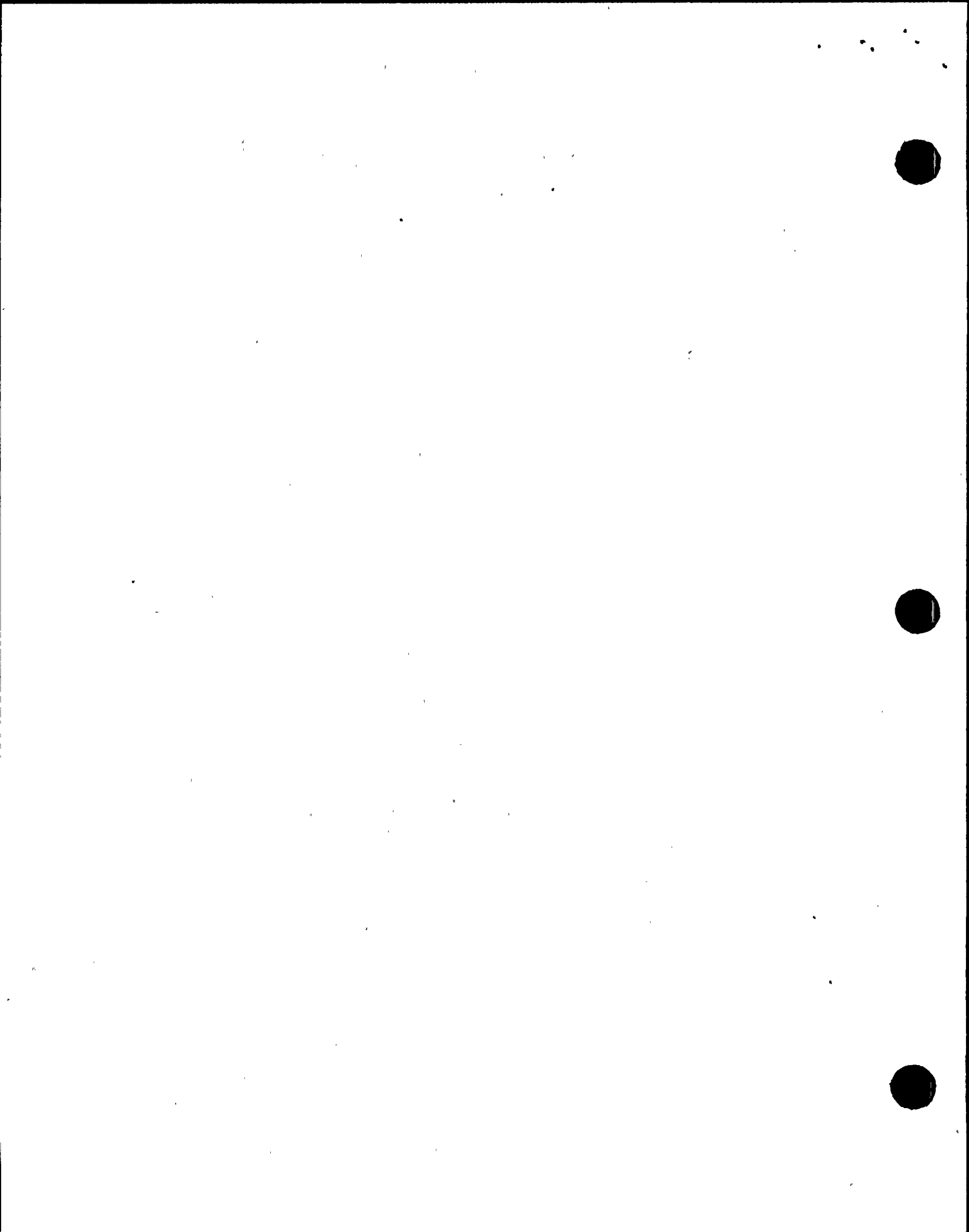


FIGURE 6-1

ASSEMBLY POWER DISTRIBUTION FOR 53 CHANNEL MODEL FOR SURRY CORE

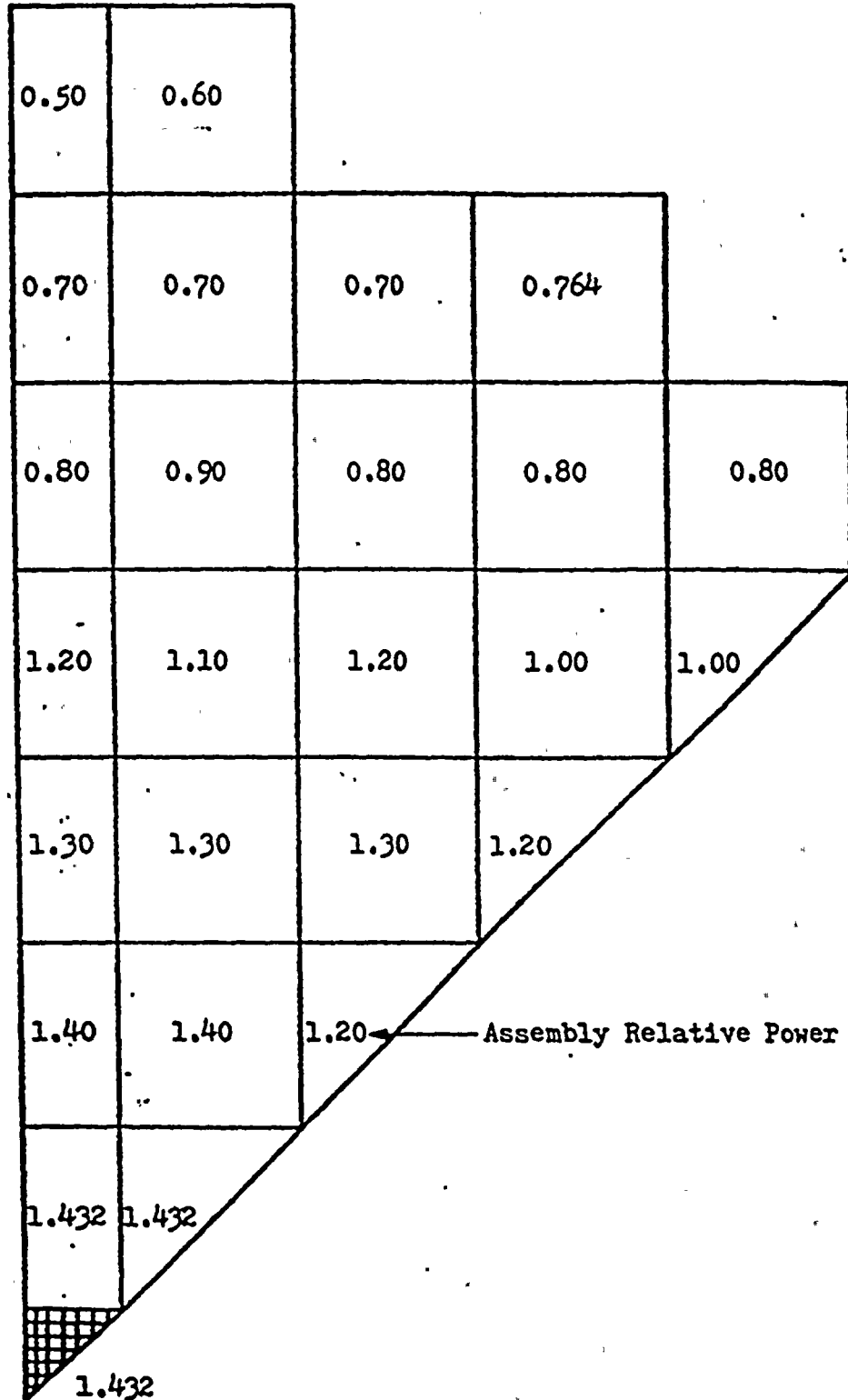


FIGURE 6-2

SUBCHANNEL POWER DISTRIBUTION FOR SURRY CORE

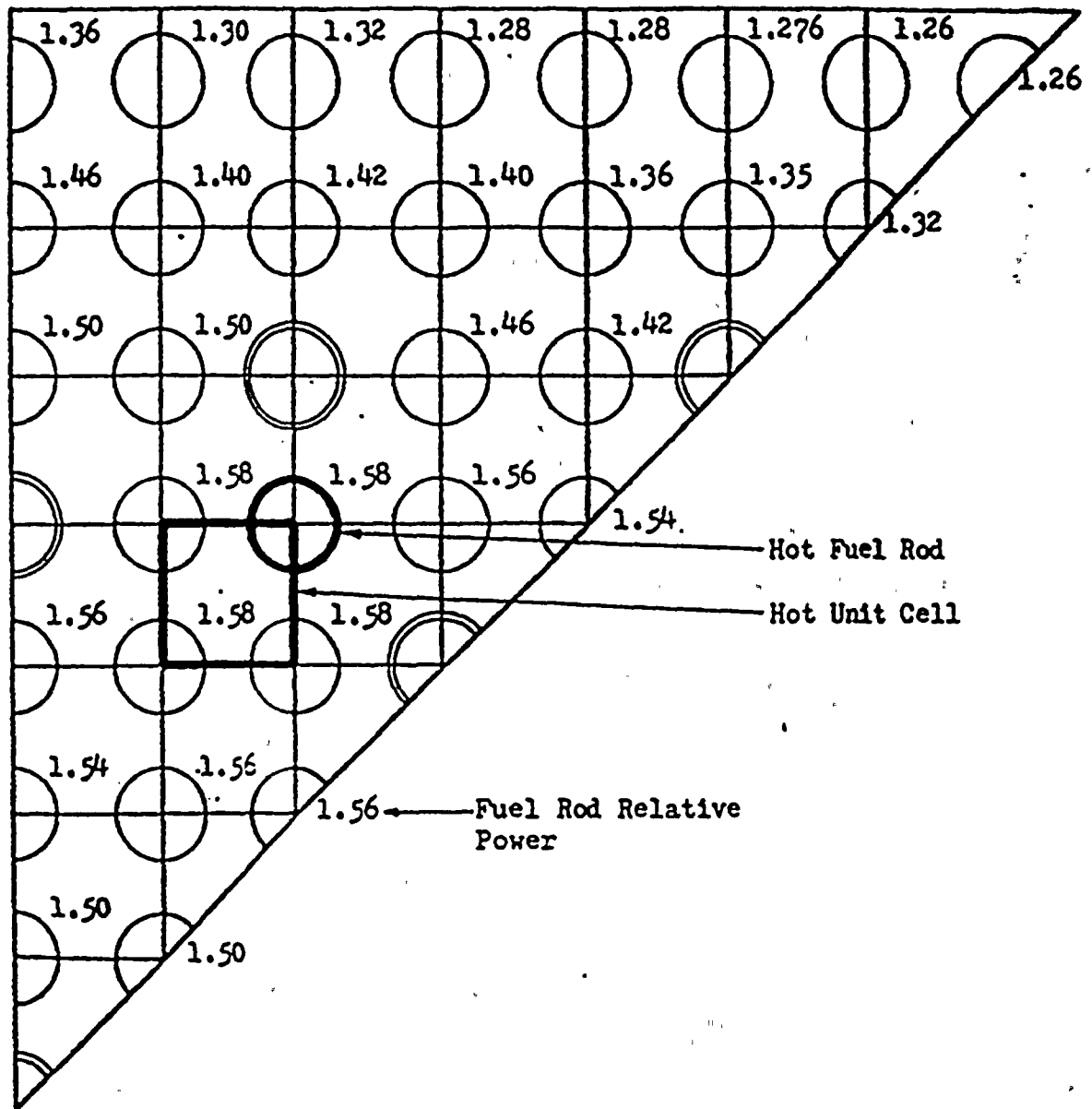


FIGURE 6-3

ASSEMBLY POWER DISTRIBUTION FOR 58 CHANNEL MODEL FOR COOK, UNIT 1 CORE

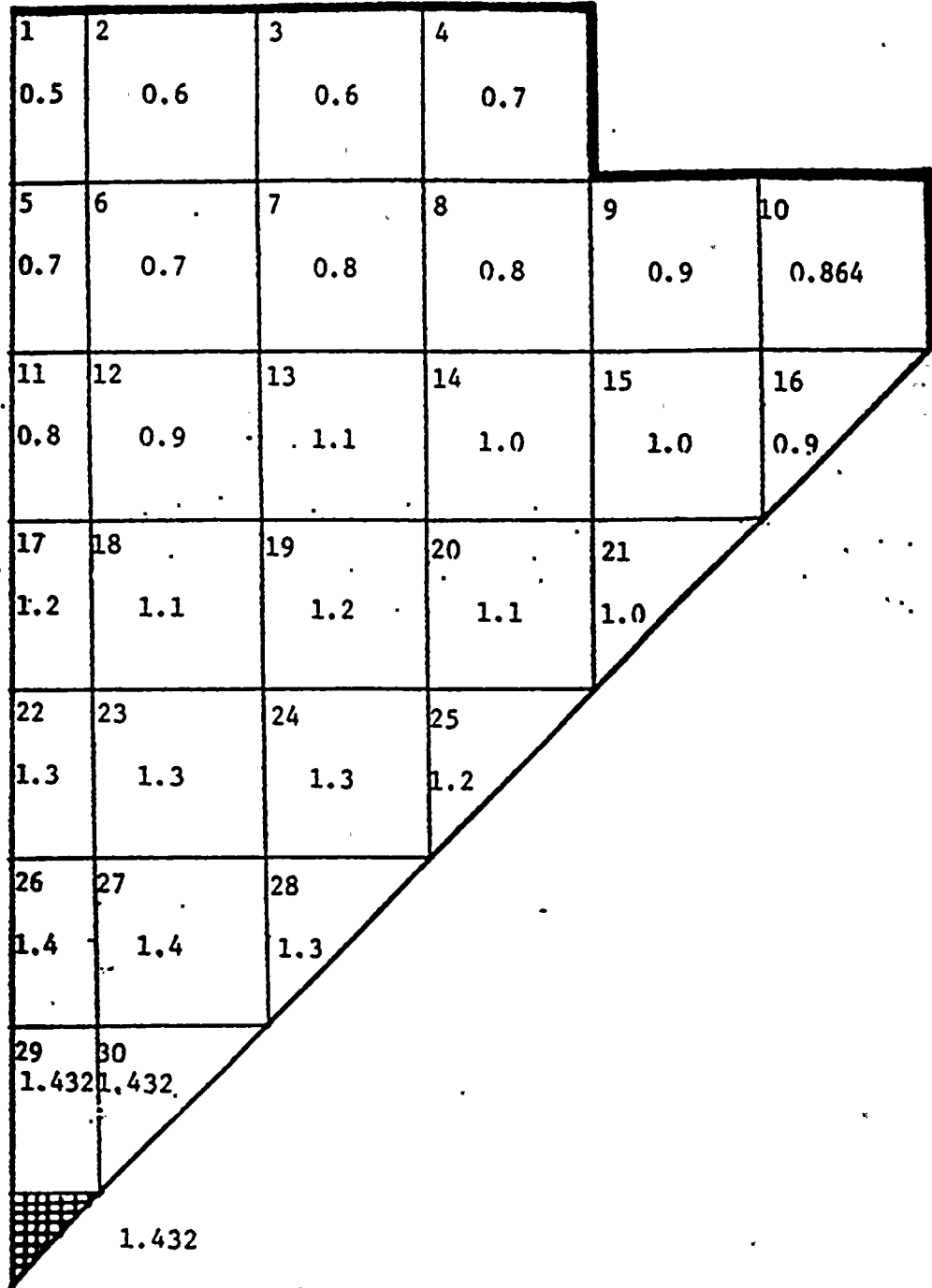


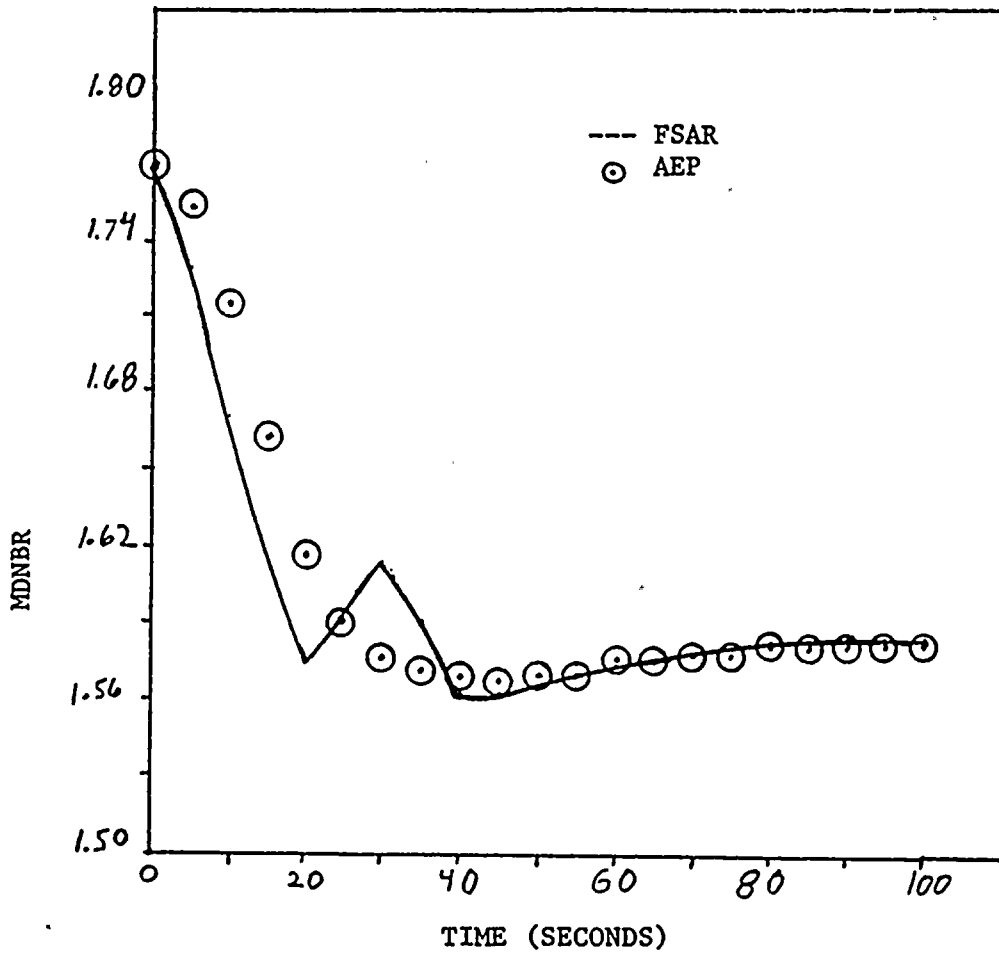


FIGURE 6-4

DNBR VS TIME

EXCESSIVE LOAD INCREASE TRANSIENT

UNIT 1, CYCLE 1 FSAR ANALYSIS



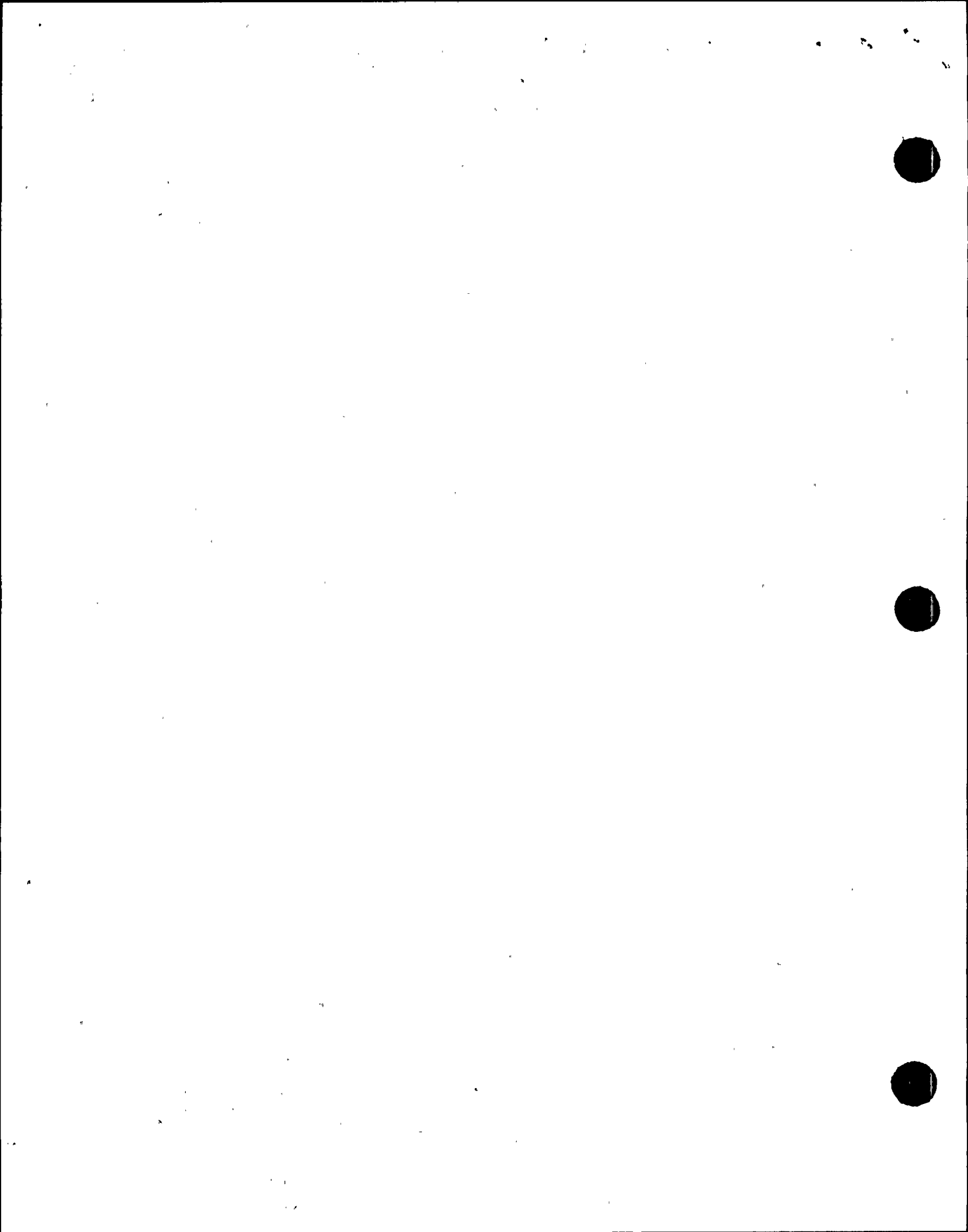
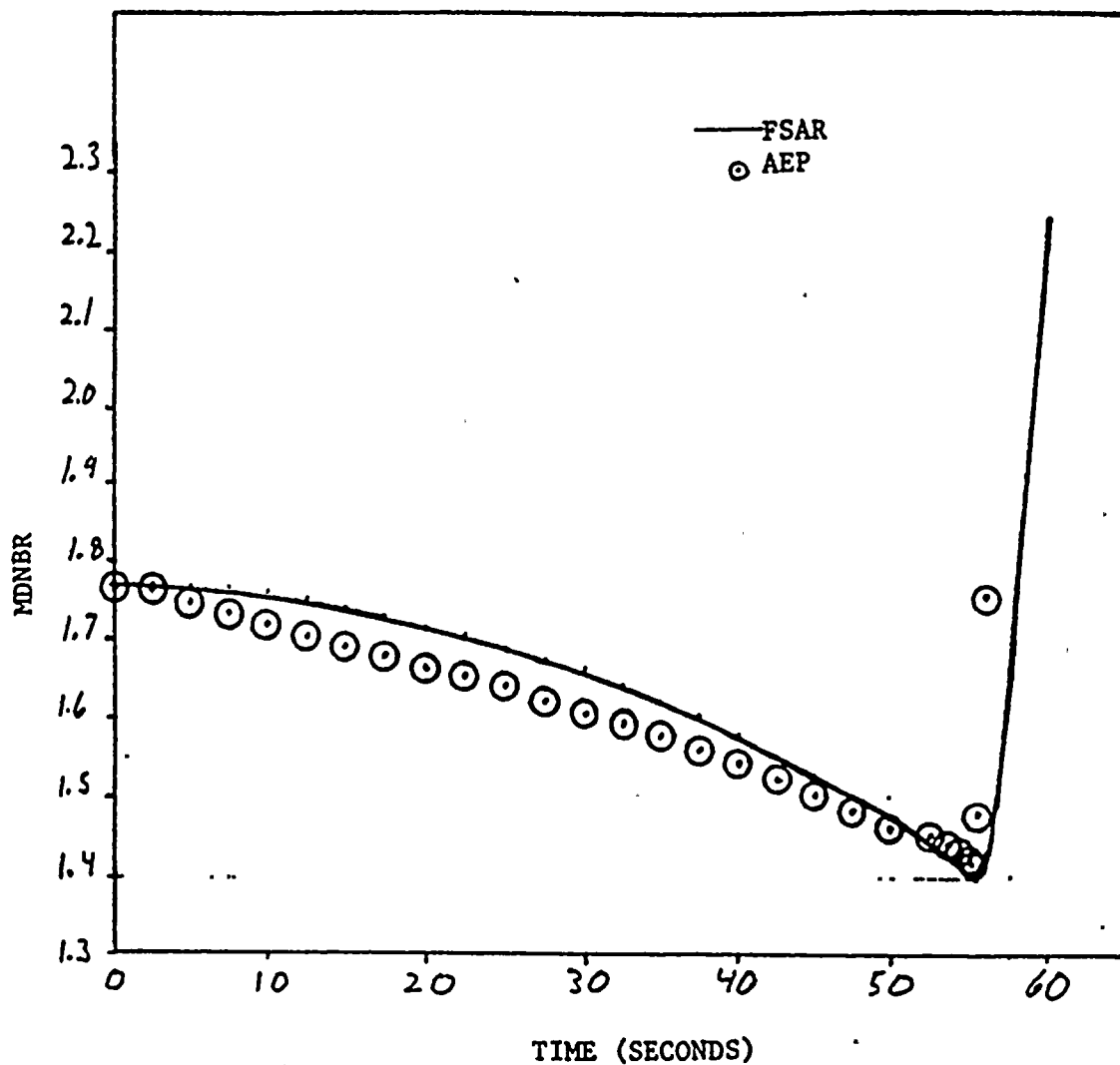


FIGURE 6-5

DNBR VS TIME

UNCONTROLLED CONTROL ROD ASSEMBLY WITHDRAWAL AT POWER TRANSIENT

UNIT 1, CYCLE 1 FSAR ANALYSIS



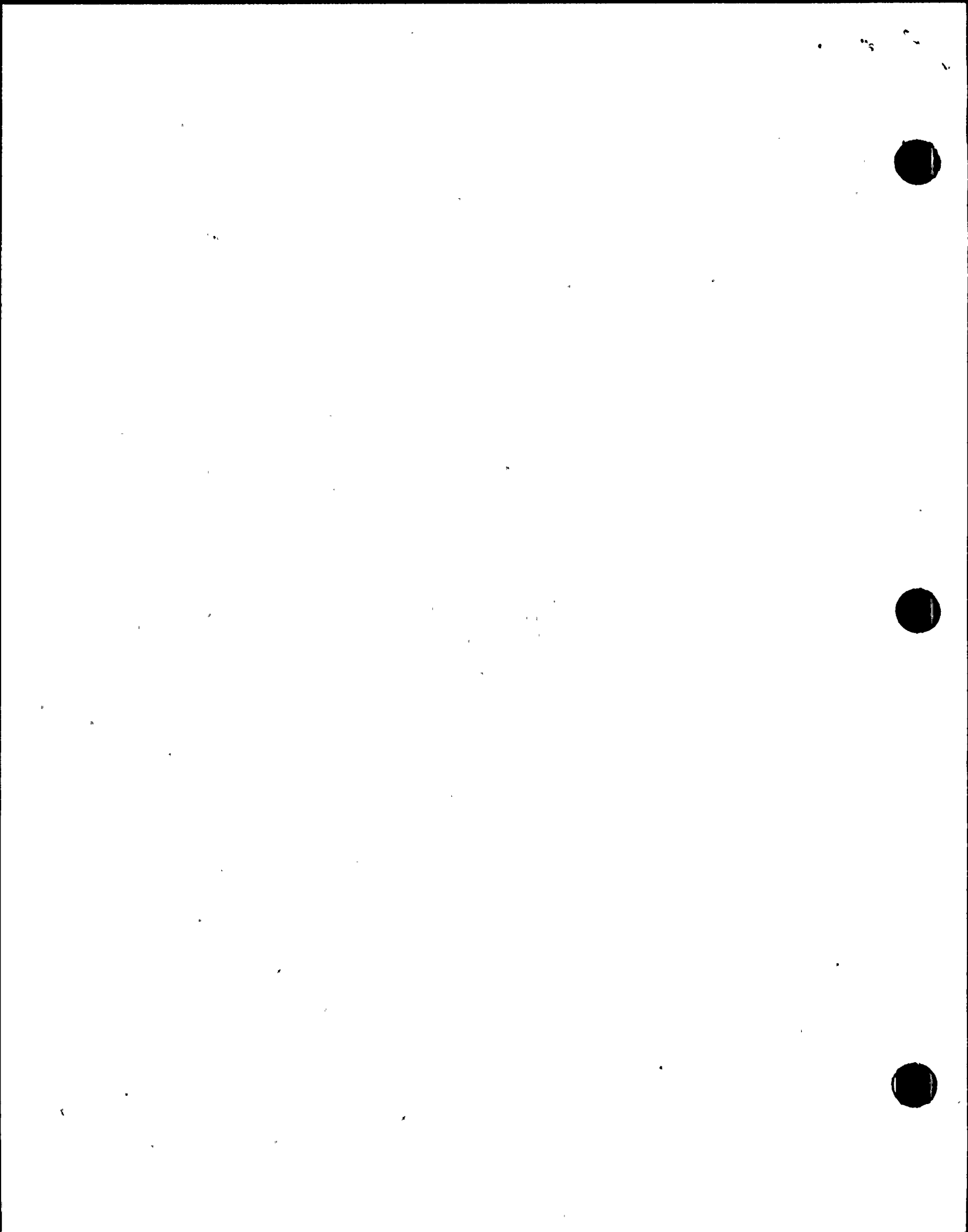
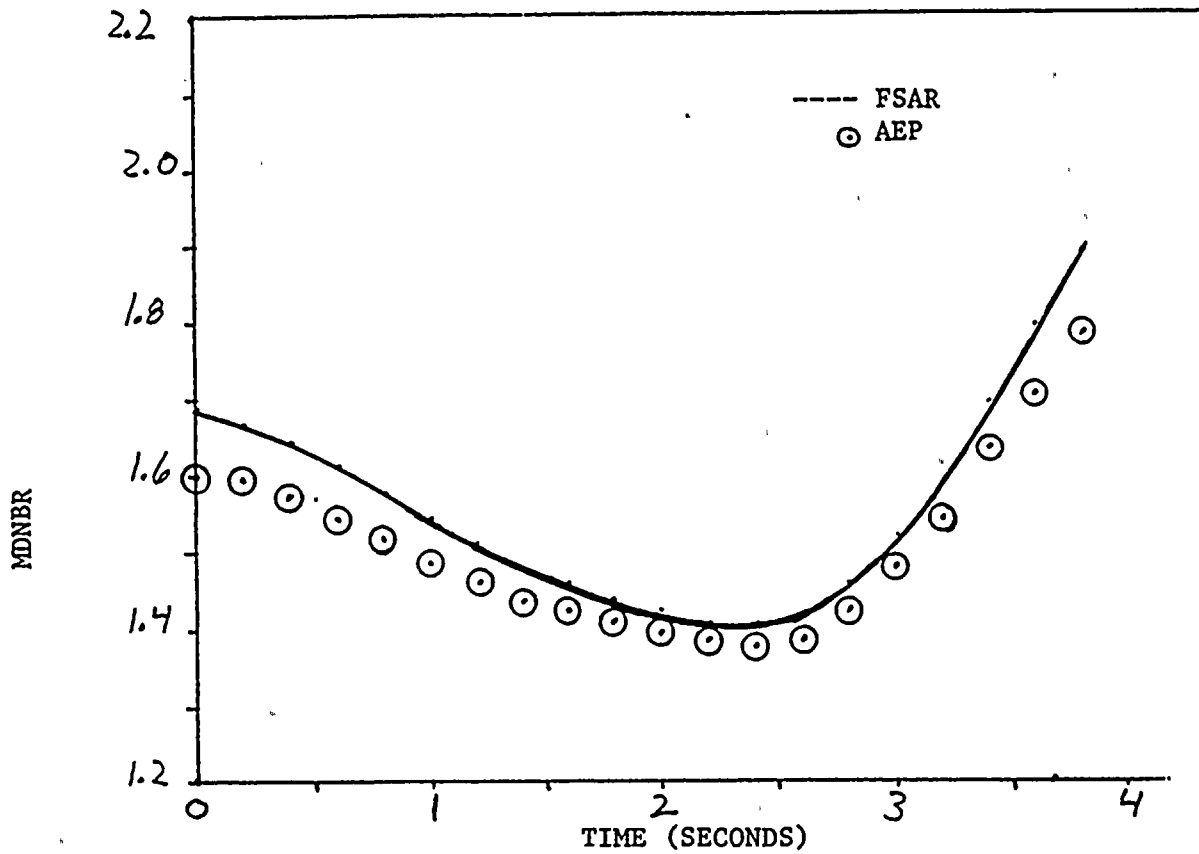


FIGURE 6-6

DNBR VS TIME

COMPLETE LOSS OF REACTOR COOLANT FLOW TRANSIENT

UNIT 1, CYCLE 1 FSAR ANALYSIS





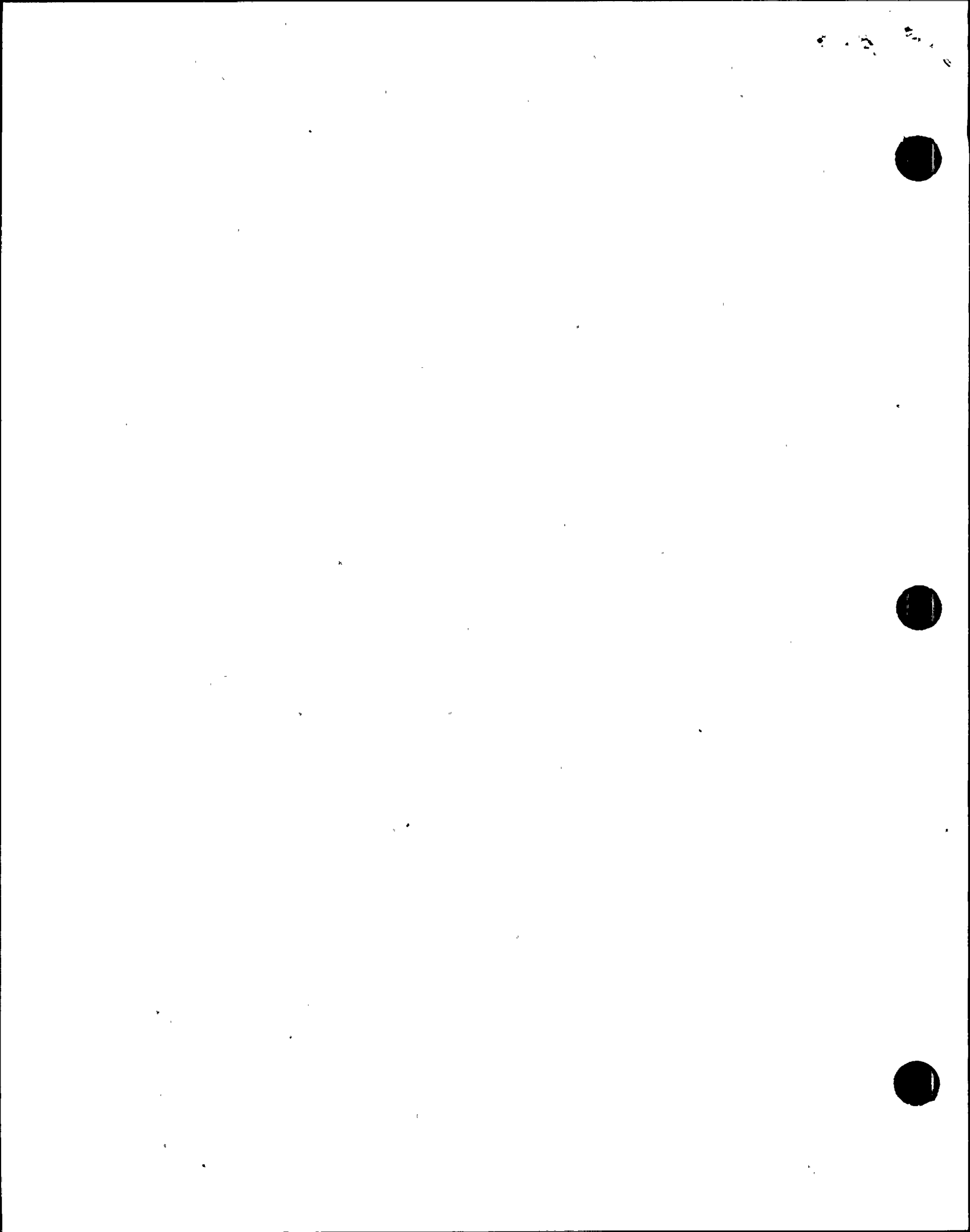
## SECTION 7

### SUMMARY AND CONCLUSIONS

American Electric Power Service Corporation has developed the core thermal-hydraulic analysis capabilities using COBRA IIIC/MIT-2 computer code. The thermal and hydraulic models, and methods developed have been documented in this report. The accuracy of the thermal-hydraulic model developed has been verified through comparisons with existing analyses and those used in the FSAR of Unit 1 of the Donald C. Cook Plant. These comparisons are summarized in Table 7-1. These comparisons indicate that the MDNBR results obtained using the AEP methodology are in excellent agreement with those presented in the licensing documents. This agreement indicates that the capability can be used to provide design and licensing support for Cook reactor operations.

TABLE 7-1  
SUMMARY OF COMPARISONS

<u>Steady State Analyses</u>	<u>Minimum DNBR</u>	
	<u>Utility/Vendor</u>	<u>AEP</u>
Surry Plant	1.94 (VEPCO)	1.90
Westinghouse 3-Loop PWR	1.985 (ANF)	1.86
Cook, Unit 1, Cycle 1	1.97 (FSAR)	1.93
 <u>Transient Analyses for Cook, Unit 1, Cycle 1 (FSAR)</u>		
	<u>FSAR</u>	<u>AEP</u>
Excessive Load Increase	1.56	1.57
Uncontrolled CRA Withdrawal at Power	1.40	1.42
Complete Loss of Reactor Coolant Flow	1.40	1.38



## SECTION 8

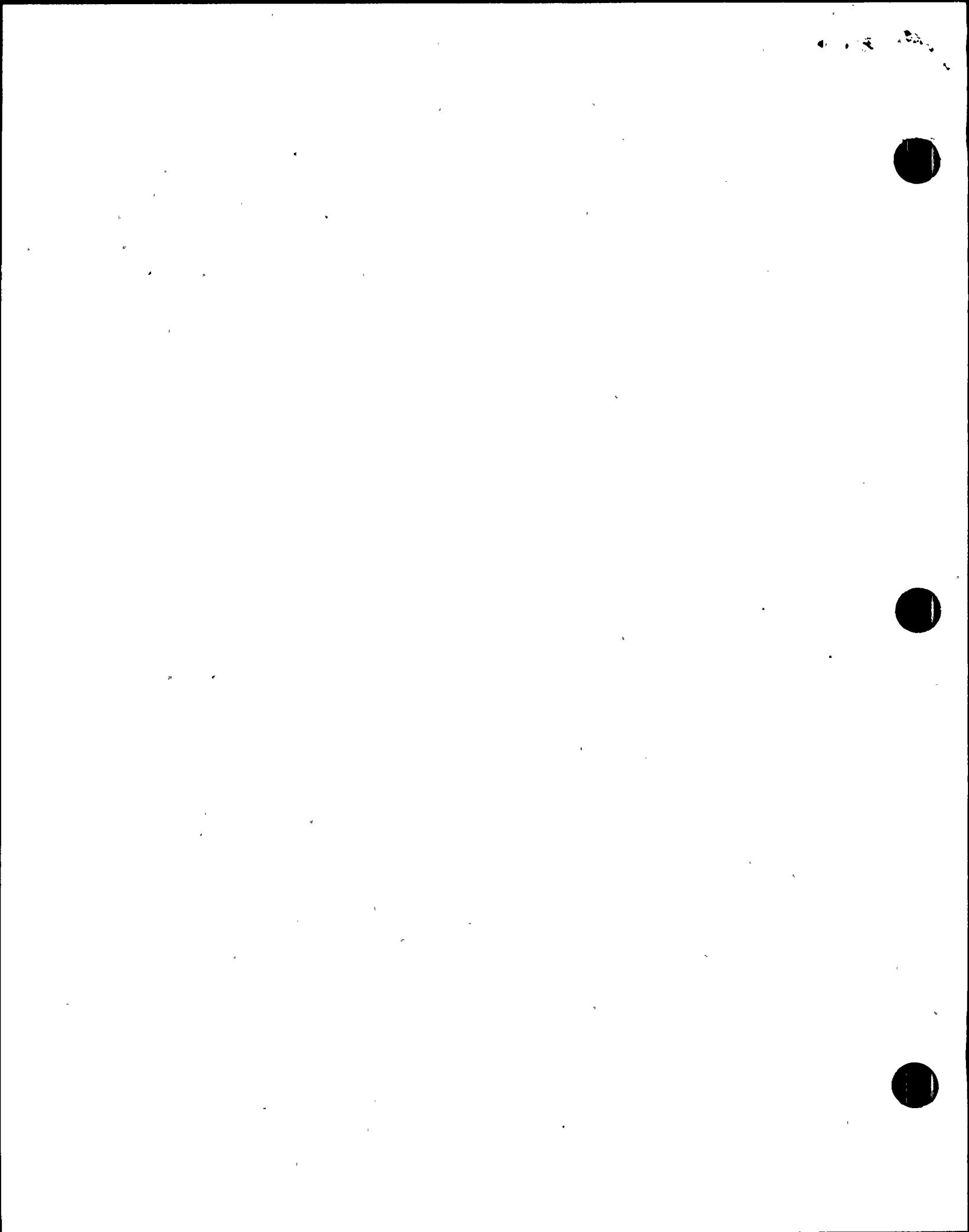
### REFERENCES

1. P. Moreno, J. Liu, E. Khan, and N. Todreas, "Steady-State Thermal Analysis of PWRs by a Simplified Method," Transactions of the American Nuclear Society, Vol. 26, p. 465, June 1977.
2. F. W. Sliz, and K. L. Basehore, "VEPCO Reactor Core Thermal-Hydraulic Analysis using the COBRA IIIC/MIT Computer Code," Virginia Electric and Power Company, Report No. VEP-FRD-33-A, October 1983.
3. T. W. Patten, et. al, "PWR Thermal-Hydraulic Hot Channel Calculations," Exxon Nuclear Co. Report No. XN-75-42, July 25, 1975.
4. Final Safety Analysis Report-Donald C. Cook Nuclear Plant, Unit 1, Indiana & Michigan Electric Company, American Electric Power System, Amendment 55, August 1974.
5. J. W. Jackson, and N. E. Todreas, "COBRA IIIC/MIT-2: A Digital Computer Program for Steady State and Transient Thermal-Hydraulic Analysis of Rod Bundle Nuclear Fuel Elements," Massachusetts Institute of Technology, Energy Laboratory Report No. MIT-EL 81-018, June 1981.
6. D. S. Rowe, "COBRA IIIC: A Digital Computer Program for Steady State and Transient Thermal-Hydraulic Analysis of Rod Bundle Nuclear Fuel Element," Pacific Northwest Laboratory Report No. BNWL-1695, March 1973.
7. L. S. Tong, "Pressure Drop Performance of a Rod Bundle," Heat Transfer in Rod Bundles, ASME, pp. 57-69, 1968.
8. F. W. Dittus, and L. M. K. Boelter, "Heat Transfer in Automobile Radiators of the Tubular Type," University of California Publications in Engineering, Vol. 2, p. 443, 1930.
9. S. Levy, "Forced Convection Subcooled Boiling-Prediction of Vapor Volumetric Fraction," General Electric Company Report No. GEAP-5157, Atomic Power Equipment Department, San Jose, California, April 1966.
10. "Plant Transient Analysis for D. C. Cook, Unit 2 with 10% Steam Generator Tube Plugging," Exxon Nuclear Company Report No. XN-NF-85-64(P), Revision 1, March 1986.

100-100000



11. Final Safety Analysis Report-Donald C. Cook Nuclear Plant, Indiana & Michigan Electric Company, American Electric Power System, Amendment 17, 1971, page 14.1-2.
12. J. M. Hellman, "Fuel Densification Experimental Results and Model for Reactor Application," WCAP-8219-A, Westinghouse Electric Corporation, March 1975.
13. Final Safety Analysis Report-Donald C. Cook Nuclear Plant, Indiana & Michigan Electric Company, American Electric Power System, Amendment 55, August 1974, Table 3.2.2-2.



2010



100-100000-100000

